Sudan University of science &Technology

College of graduate studies and scientific research

Assessment of Radiation Dose of Pediatric and Adult patients for Computed Tomography Examination

تقييم الجرعات الاشعاعية للاطفال و الكبار من المرضي في فحوصات الاشعة المقطعية

A thesis Submitted for Fulfillment as a Requirement of PhD Degree in medical physics

By:

Rufida Elbushra Eisa Ahmed

Supervisor:

Dr. Mohamed Elfadil Mohamed

Co-supervisor:

Ikhlas Abdalaziz Ahmed

July 2019

الآية

قال تعالى:

{ اقرأ باسم ربك الذي خلقَ}

العلق 1

Dedication

To those whom I always found in better or worse thank you,

Mother, Brother and my Husband …. The light of my life.

Acknowledgement

- To ALLAH am thank full for guiding and enlighten my insight whenever the darkness or mistake are found.

- Am deeply great full to my mentor Prof. **Mohamed Alfadil** for his Patience, kindness, guidance and assistance in teaching me throughout the whole period of this study.

- To those who lay there hands for me M. Salman (Iben Alhitham), M. Mhutady and M. Abdallatef (Alyaa hospital) , Suheeb am deeply tank full for their help.

Content

List of figures

List of abbreviations

CT: Computed Tomography

CAT: Computed Axial Tomography.

CTA: Computed Tomography Angiography.

ALARA: As Low As Reasonably Achievable.

Equiv.D: Equivalent Dose.

Eff.D: Effective Dose.

mSv: milli Sievert **.**

mGy: milli Gray**.**

CTDI: Computed Tomography Dose Index.

DLP: Dose Length Product.

MDCT: Multi Detector Computed Tomography.

MSCT: Multi slice Computed Tomography.

SSCT: single slice Computed Tomography.

Abstract

The important of this study comes from the increased number of CT procedures to adult and pediatric as CT consider invasive investigation. Patient data for both male and female collected from four different hospital and centers in Khartoum which using different CT scanner modalities. The data of this study were collected from Alya Hospital (Toshiba, 64 slice), Ibn Alhitham specialist (Toshiba, 4 slice), Alzytouna Hospital (Toshiba, 64 slice) and Modern center (GE, 16 slice). it preformed for brain and chest in adult and pediatric patients Comparing the dose parameters among the two exams for all hospitals for brain the CTDIvol, DLP and ED was 76.82 ± 16.07, 2199.45 ± 1789.7 and 4.62 ± 3.76 respectively, while for CT chest was 32 ± 11.33, 837.59 ± 338.54 and 11.75 ± 4.8 respectively in adults. When Comparing the dose parameters(CTDIvol, DLP and ED) among the two exams for all hospitals for brain the CTDIvol, DLP and ED was 53.4 ± 9.7, 861.9 ± 268 and 7.58 ± 2.83 respectively, while for CT chest was 8.69 ± 2.78, 302.22 ± 161.75 and 7.8 ± 4.05 respectively for pediatric. Finally the radiographic data show that ED for adult male were higher than adult female as it is for pediatric male expect the CTDIv were higher for pediatric females than males.

الملخص

تاتي اهمبه هذه الدراسة نسبة لزياده عدد فحوصات الاشعة المقطعية للبالغين و الاطفال .قد جمعت بيانات هذه الدراسه من ثلاث مستشفيات و مركز داخل ولايه الخرطوم ، و هي مستشفي علياء التخصصي(توشيبا 64 شريحة)، مستشفي ابن الهيثم(توشيبا 4 شرايح)، مستشفي الزيتونه((توشيبا 64 شريحةe) و المركز الطبي الحديث(جنرال الكتريك 16 شريحة) اجريت هذه الرراسة علي فحصي الراس و الصدربالنسبه للبالغين و الاطفال عند مقارنه العوامل المؤثره علي الجرعة لهذين العضوين نجد ان المعطيات بالنسبة لفحص الراس كالتالي (حجم مؤشر جرعة التصوير المقطعي ,جرعة ناتج الطول ,الجرعة المكافئة 76.82 ± 16.07, 2199.45 ± 3.76 ,4.62 ± 1789.7) و لفحص الصدر (حجم مؤشر جرعة التصوير المقطعي ,جرعة ناتج الطول ,الجرعة المكافئة4.8 ± 11.75 , 338.54 ± 837.59 ,11.33 ± 32) هذه المعطيات بالنسبة للبالغين. اما بالنسية للاطفال فقد كانت العوامل المؤثره علي الجرعة بالنسبة لفحص الراس كما يلي (حجم مؤشر جرعة التصوير المقطعي ,جرعة ناتج الطول , الجرعة المكافئة,2.83 ± 7.58 , 268 ± 861.9 ,9.7 ± 53.4) و لفحص الصدر كالتالي(حجم مؤشر جرعة التصوير المقطعي ,جرعة ناتج الطول ,الجرعة المكافئة ± 302.22 ,2.78 ± 8.69 (161.75 ,7.8 ± 4.05

Chapter one

Introduction

1.1 Introduction

1.1.1 Computed Tomography (CT) Imaging

Johann Radon showed in 1917 that 2-D section images could be reformulated using mathematical transformation of projection data (i.e. using a Radon transform). Projection data are line integrals (summations of image values) recorded across an object at some angle. The link between projection data and x-ray images (maps of the effects of attenuation) was not obvious. However, motivation was high since section x-ray images would have the ability to make high contrast section images of the body by removing interference from overlapping tissues. Later in this chapter we will see how the projection dilemma was resolved. Even with the knowledge of how to make x-ray images into projections, imaging instrumentation and computing power was not able to provide this capability early on, so we had to wait many years for technology to catch up with the theory.

By the 1960s several research labs were able to reconstruct x-ray section images from x-ray projections acquired from physical objects, and these successes spurred intensive research into devices that could be used in humans. In the 1970s x-ray computed tomography (CT) was formally introduced for clinical use, which was followed by rapid technological refinement. Since reconstructed images looked like the thinly sliced tissue sections used for microscopic inspection, the term "Tomography", literally meaning a picture of a cut section, was adopted and early x-ray tomographic imaging systems were called Computed Axial Tomographic or “CAT” scanners. However, common use has dropped this designation in favor of

computed tomography or just CT. In 1979 two early researchers in the field, A. M. Cormack and Godfrey Hounsfield (Hunold *et al.* 2003).

1.1.2 Computed Tomography X-ray System in Medicine

Computed Tomography (CT) was invented by a British engineer, Sir Godfrey Hounsfield who also won the Nobel Prize because of his invention. CT was first introduced in the clinical practice in 1972 which was only limited to the brain scan. Prior to that, X-ray planar radiography and fluoroscopy systems were the main contributors of radiation in imaging (Goldman 2007). CT has fascinated the world with production of high contrast resolution images for visualizing soft tissues and the ability of producing tomographic and three dimensional (3D) volumetric images (IAEA 2007). Thus, it has changed the perception on medical diagnostic quality and as a result it has improved the quality of healthcare. Now, CT is becoming a common diagnostic tool in many major hospitals in the whole world. It is obvious that CT gives a lot of advantages such as faster scanning procedure, good spatial resolution and good contrast, compared to other modalities. Nowadays, many medical centres choose to send cases like accident and emergency cases, urology, cardiac imaging and pediatric imaging for CT scan as their first option for easy diagnosis of the symptoms. In some countries, sinusitis cases were likely referred to CT compared to the plain radiograph because CT were able to show important structures (Zammit-Maepel *et al.* 2003). Having taken notice of that, the manufacturers are also intense in introducing the latest technologies and applications of their CT due to the high demand of the CT scanners. This can be seen in Figure 1.3 where the number of CT scanners installed in Germany has increased linearly (Nagel 2000). Drastic increase happened after 1990 when the helical CT was introduced to the market.

1.1.3 Radiation Issues in Computed Tomography

The distribution of X-ray in CT is different from planar radiography. In CT, a complete scan consists of thousands of radiation beams projected in circular directions around the object. It is very obvious that CT imparts relatively higher radiation dose than planar radiography. For example, a single routine CT of the chest has been identified to give radiation equivalent dose of 400 planar radiography of the chest (Rehani and Berry2000).

Council of European Union (1997) has clearly stated in the Council Directive 97/43/EUROTOM (June 1997) that CT produces the radiation as high as that of interventional radiology and radiotherapy:*"Member States shall ensure that appropriate radiological equipment, practical techniques and ancillary equipment are used for the medical exposure- of children, - as part of a health screening programme,- involving high doses to the patient, such as interventionalradiology, computed tomography or radiotherapy."*

The increase number of CT scanners installed worldwide has led to drastic increase of CT examinations. The contribution of radiation dose from CT examinations to the patients also increases and this has caused anxiety to the radiological communities. In the UK, it has been reported that CT constituted only about 2-3% of all radiological examination but it has contributed 20-30% to the total radiation dose in medical practices (Shrimpton *et al.* 1991). Until 10 years ago, there was about 35% increase of radiation dose from CT of the abdomen and pelvis in the UK (Wall and Hart 1997) and this increase has made substantial impact on the patient care and, patient and population exposure from medical X-ray (European Commission 2005). In the US, although CT comprised approximately 10% of total diagnostic radiological procedures, but it contributes approximately 65% of the effective radiation dose to the

total national medical X-ray examinations (Mettler *et al.* 2000, National Cancer Institute 2002). Based on the United Nations Scientific Committee on the Effects of Atomic Radiation report (UNSCEAR 2000), there was about 20% increase of global collective dose for 5 years 8 period (1985 to 1990 and 1991 to 1996). The number of CT examinations on children is also increasing. It has been reported that 2 – 3 millions of the CT examinations were performed on children every year (National Cancer Institute 2002, Rehani and Berry 2000). Noteworthy, children are more sensitive to the radiation than adults as their growth rates are faster. New advancement of the CT has also led to great increase of the radiation dose to the patients. The use of multi-slice computed tomography (MSCT) has aggravated the scenario with the increasing of collective dose of CT examinations because the MSCT produces higher dose to the patients compared to single slice CT (SSCT) (Hunold *et al.* 2003).

1.2 Classification of Radiation

Radiation is classified into two main categories, as shown in Fig. 1.1: *nonionizing* and *ionizing*, depending on its ability to ionize matter. The ionization potential of atoms, *i.e.*, the minimum energy required for ionizing an atom, ranges from a few eV for alkali elements to 24.6 eV for helium (noble gas).

• *Non-ionizing radiation* cannot ionize matter because its energy is lower than the ionization potential of matter.

• *Ionizing radiation* can ionize matter either directly or indirectly becauseits energy exceeds the ionization potential of matter. It contains two major categories:

– *Directly ionizing radiation* (charged particles, *electrons, protons, alpha particles, heavy ions)*

– *Indirectly ionizing radiation* (neutral particles) *photons (x rays, gamma rays), neutrons*

-*Directly ionizing radiation* deposits energy in the medium through direct Coulomb interactions between the directly ionizing charged particle and orbital electrons of atoms in the medium.

Indirectly ionizing radiation (photons or neutrons) deposits energy in the medium through a two step process:

• In the first step a charged particle is released in the medium (photons release electrons or positrons, neutrons release protons or heavier ions).

• In the second step, the released charged particles deposit energy to the medium through direct Coulomb interactions with orbital electrons of the atoms in the medium. Both directly and indirectly ionizing radiations are used in treatment of disease, mainly but not exclusively malignant disease. The branch of medicine that uses radiation in treatment of disease is called *radiotherapy*, *therapeutic radiology* or *radiation oncology*. *Diagnostic radiology* and *nuclear medicine*

1.3 Health Effects from Exposure to Ionizing Radiation

The individual risk from radiation associated with a CT scan is quite small compared to the benefits that accurate diagnosis and treatment can provide. Still, unnecessary radiation exposure during medical procedures should be avoided. Unnecessary radiation may be delivered when CT scanner parameters are not appropriately adjusted for the patient size (Anne et al. 2001). In conventional X-ray procedures, medical personnel can tell if the patient has been overexposed because of the film is overexposed, producing a dark image (ICRP 2006). However, with CT there is no obvious evidence that the patient has been overexposed because the quality of the image may not be compromised. Several recent articles (Kalender et al. 1999, Rehani,

Berry 2000) stress that it is important to use the lowest radiation dose necessary to provide an image from which an accurate diagnosis can be made, and that significant dose reductions can be achieved without compromising clinical efficacy.

The United Nation Scientific Committee on the Effects of Atomic Radiation (UNSCEAR, 2000) has highlighted that the worldwide there about 93 million CT examinations performed annually at a rate of about 57 examinations per 1000 persons. UNSCEAR also estimated that CT constitutes about 5% of all X-ray examinations worldwide while accounting for about 34% of the resultant collective dose. In the countries that were identified as having the highest levels of healthcare, the corresponding figures were 6% and 41% respectively.

The doses tissues from CT can often approach or exceed levels known to increase the probability of cancer, technologists are responsible for managing the dose in collaboration radiologists and medical physicists, CT examinations are increasing in frequency, newer CT techniques have often increased doses when compared with standard CT, referring physicians and radiologists should make sure that the examination is indicated and many practical possibilities currently exist to manage dose. The most important is reduction in mA.

1.4 Problem of the study

Different protocol and different type of machine give different dose for pediatric and adult, increasing radiation hazard for pediatric due to active cellular division affect their life spam, that why we need to make reference dose for both pediatric and adult in order to ass the effective radiation dose and find a standard reference dose level.

1.5 Objective

The general objective of this study is to assess the radiation dose for pediatric and adult in CT examination.

1.6 Specific objectives

- To measure the dose parameter DLP, CTDIv for adult and pediatric.
- To calculate the effective dose for adult and pediatric.
- To compare the effective dose for adult and pediatric.
- To compare the dose parameter between different hospitals.
- To differentiate between imaging protocol for adult and pediatric.
- To compare the present study with international studies and organization.

1.7 Thesis outline:

This study will be consisted of five chapters, with chapter one is an introduction which, includes; objectives, problem of the study and importance of the study. While chapter two will includes a comprehensive literature review, and chapter three will describe the material and method. Chapter four will include result presentation; finally chapter five will include the discussion and conclusion.

Chapter Two

Section one

Theoretical Background

2.1 Computed Radiography (CT) Equipments and Generations

A CT system comprises several components. These basically include:

- The scanning unit, i.e. the gantry, with tube and detector system.
- The patient table.
- The image processor for image reconstruction.
- The console.

The console represents the man-machine interface and is designed to be Multifunctional. It is the control unit for all examination procedures, and is also used to evaluate the examination results. To enhance the workflow, Siemens has developed a double console capable of performing both functions at the same time (CT History and Technology, 2011).

2.1.1 Scanning unit (gantry)

A CT scanning system consists of an X-ray unit, which functions as a transmitter, and a data acquisition unit, which functions as a receiver. In commercial CT systems these two components are housed in a ring shaped unit called the gantry.

2.1.1.1 X-ray components

Tube Manufacturers of CT systems use X-ray tubes with variable focal spot sizes. This makes sense, because volumes for which good low-contrast resolution is essential need to be scanned with a large focal spot and high power, whereas high resolution images with thin slices require a small focal spot. Tubes used in modern CT scanners have a power

rating of 20–60 kW at voltages of 80 to 140 kVp. The systems can, however, be operated at maximum power for a limited time only. These limits are defined by the properties of the anode and the generator. To prevent overloading of the X-ray tube, the power must be reduced for long scans. The development of multi-row detector systems has practically excluded this limitation, since these detector systems make much more efficient use of the available tube power (CT History and Technology, 2011).

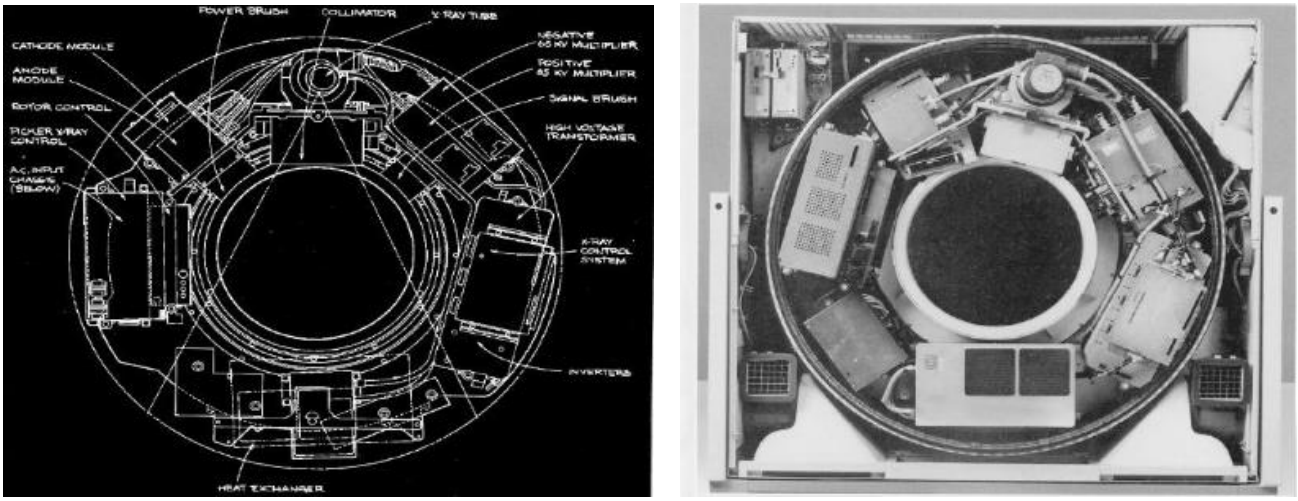

Fig 2.1 The major internal components of afourth-generation CT gantry are shown in a photograph with the gantry cover removed (A) and identified in the line drawing (B)

Shielding Each CT scanner is equipped with grids, collimators and filters to provide shielding against scattered radiation, to define the scan slice and to absorb the low-energy portion of the X-ray spectrum. In this way, both the patient and the examiner are protected (CT History and Technology, 2011).

2.1.1.2 Data acquisition components

Detector The detector system plays a special role in the interaction of the CT components. It converts the incident X-rays of varying intensity to electric signals. These analog signals are amplified by downstream electronic components and converted to

digital pulses. Over time, certain materials have proven very effective in the utilization of X-rays (CT History and Technology, 2011).

Multi-row detector Multi-row detectors utilize radiation delivered from the X-ray tube more efficiently than single-row detectors. By simultaneously scanning several slices, the scan time can be reduced significantly or the smallest details can be scanned within practicable scan times. In the adaptive array detectors, the rows inside the detector are very narrow, becoming wider as you move toward its outer edges in the z direction interconnection provides considerable flexibility in the selection of slice thicknesses. At the same time the space required by the detector septa, and therefore the space, is minimized (CT History and Technology, 2011).

2.1.1.3 Scanner Parameters

Collimation

The radiation beam emitted by the X-ray tube is shaped using special diaphragms also referred to as ”collimators”. A distinction can be made between two types of collimators .The source collimator is located directly in front of the radiation source – i.e. the X-ray

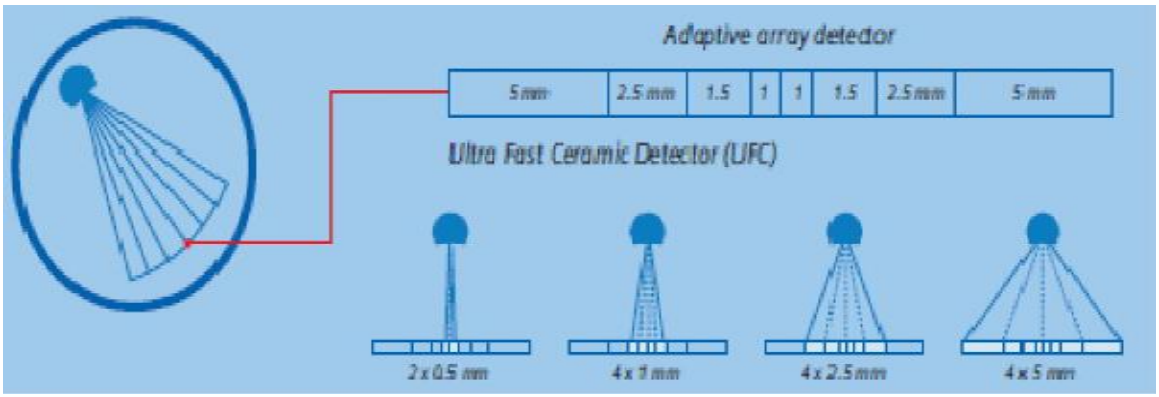

Fig 2.2 variable slice collimation through primary collimation and electronic signal combination.

tube. It reduces the radiation beam to form the maximum required fan beam, thus also determining the emitted dose. The detector collimator, which is positioned directly in front of the detectors, is primarily used to shield the detector against scattered radiation, thus preventing image artifacts. The collimation and focal size determine the quality of the slice profile. From the data volume from a multislice scanner images can be reconstructed with slice thickness equal to or larger than the detector collimation. For example, a 5 mm collimation allows images to be reconstructed with a slice thickness of 5 mm or more. The widest range possibilities in the selection of collimation and reconstructed slice thicknesses are offered in spiral CT using multidetector systems (CT History and Technology, 2011).

Increment The increment determines the distance between images reconstructed from a data volume. If an appropriate increment is used, overlapping images can be reconstructed. In sequential CT, overlapping images are obtained only if the table feed between two sequences is smaller than the collimated slice thickness. This, however, increases the patient dose. In spiral CT the increment is freely selectable as a reconstruction parameter, i.e. by selecting the increment the user can retrospectively and freely determine the degree of overlap without increasing the dose. Overlapping reconstructions offer the advantage of better image quality due to lower noise and easier and more accurate diagnosis of small structures. An illustrative example: A 100 mm range was acquired in the spiral mode with 10 mm collimation. After the acquisition, slices of 10 mm thickness can be reconstructed at any point of this range. If an increment of 10 mm is used, contiguous slices of 10 mm thickness are reconstructed every 10 mm 10 mm thickness are reconstructed every 5 mm. The slices overlap by 50%. With an

appropriate increment an overlap of 90% can be achieved. Modern CT systems allow the reconstruction of slices with arbitrary increment overlap is 30%–50%.

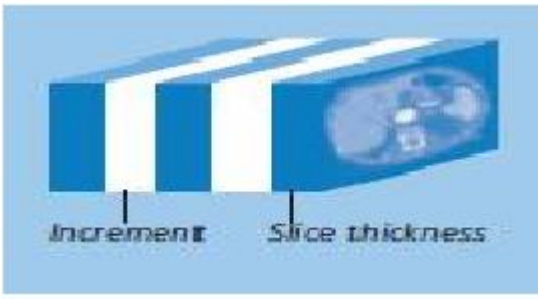

Fig 2.3(a) slice thickness

Fig 2.3(b) overlapping slices

2.1.2 The Patient Table

Pitch An important factor in spiral scanning is the table feed per rotation. The larger the table feed, the faster However, if the table feed is too large, image quality will be impaired. In this context the term "pitch" is used. For single-row systems the definition

pitch = table feed per rotation/collimation

is generally accepted. Experience has shown that a good image quality can be obtained with a pitch between 1 and 2. It should also be noted that the dose can be significantly reduced in single-row systems if a pitch factor > 1 is applied. In the context of multi-row systems, pitch cannot yet be defined clearly. The ambiguity involved becomes apparent in the following example:

Collimation 4 x 2.5 mm, table feed 10 mm

First possibility: pitch = 10 mm/4 x 2.5 mm = 1

Second possibility: pitch = 10 mm/2.5 mm = 4

To avoid misunderstandings, we use “feed per rotation“rather than “pitch“on the user interface (CT History and Technology,2011).

Rotation time Rotation time is the time interval needed for a complete 360°rotation of the tube-detector system around the patient. It affects the spiral scan length and thus the coverage of the scan range during a certain period of time. Ultra modern CT systems require only 0.4 seconds for one rotation. A short rotation time has the following advantages:

1. A longer spiral scan can be acquired in the same scan time.
2. The same volume and the same slice thickness can be scanned in less time.
3. Motion artifacts are eliminated.
4. Savings on contrast media through shorter examination times.
5. Reduced patient discomfort, since less contrast medium is required.

For shorter examination times or fast acquisition of large anatomical regions a sub second rotation time is recommended. This applies especially, for instance, to constantly moving organs such as the heart (CT History and Technology, 2011).

mAs The mAs value (e.g. 100 mAs) is the product of the tube current (e.g. 200 mA) the rotation time (e.g. 0.5 s) using what is commonly called “effective mAs”. This is the product of the tube current and the exposure time for one slice (rotation x collimation/feed per rotation) the selected mAs and tube voltage determine the dose. The mAs value selected depends on the type of examination. Higher mAs values reduce the image noise, thus improving the detect ability of lower contrasts. For visualizations of soft tissue, i.e. regions of low contrast, a higher dose and larger slice thickness are required. The abdomen and brain are typical regions of soft-tissue contrast.

Visualizations of bones or the lungs, i.e. regions of high contrast, as well as contrast studies of vessels require lower doses and thinner slices. CT scanners also feature the CARE Dose technical measures package (CARE = Combined Applications to Reduce Exposure) which was developed to reduce patient exposure to radiation. This package guarantees shorter examination times, the lowest possible exposure to radiation, and images of excellent quality. Ultra modern computer technology "monitors" the patient during the entire examination period. During each rotation, the radiation is continuously measured and modulated according to the current attenuation level. CARE Dose thus

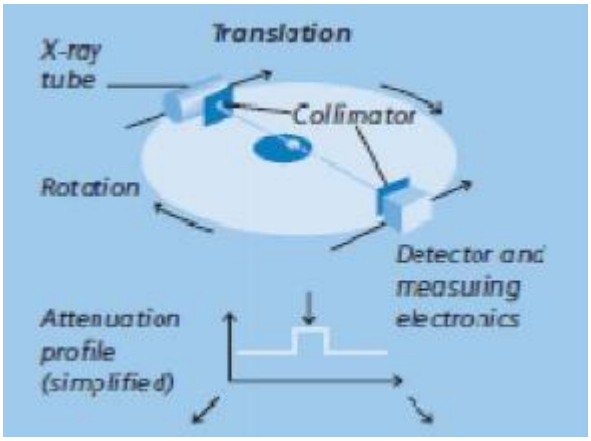

Fig 2.4 The acquisition of CT image

makes it possible to vary the radiation dose depending on the patient's anatomy and thus reduce it by as much as 56%.Scanner parameters determine the image quality. Optimal performance of spiral CT systems can be achieved only with an optimal combination of parameters (CT History and Technology, 2011).

2.1.3 The image processor for image reconstruction

Acquisition In the simplest case, the object (here a round cylinder) needle-like beam This produces a sort of shadow image (referred to as"attenuation profile" or" projection") which is recorded by the detector and the image processor. Following further rotation of

the tube and the detector by a small angle, the object is once again linearly scanned from another direction, thus producing a second shadow image. This procedure is repeated several times until the object has been scanned for a 180° rotation (CT History and Technology, 2011).

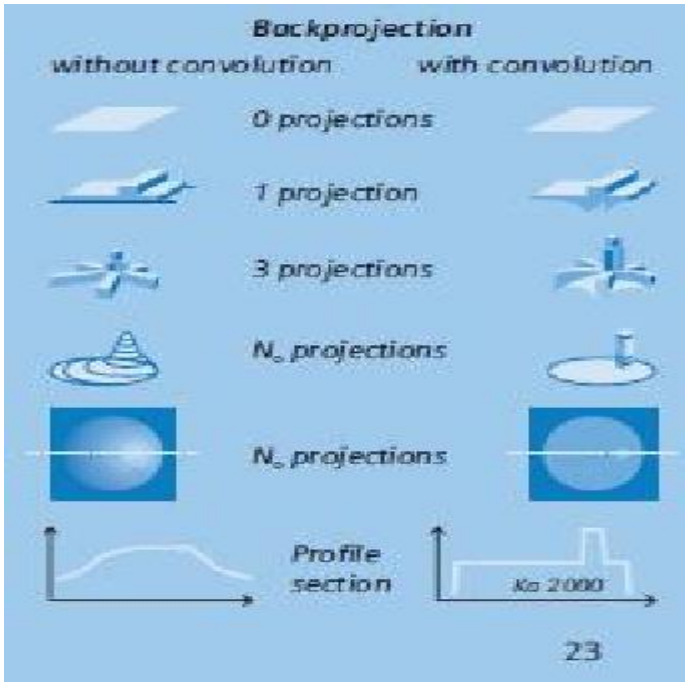

Fig 2.5 The Back projection without convolution and with convolution

Display The various attenuation profiles are further processed in the image processor. In the case of simple backprojection, each attenuation profile in the scanning direction is added up in the image memory. This result in a blurred image due to the disadvantage of this simple backprojection, i.e. each object not only contributes to its own display, but also influencesthe image as a whole. This already becomes visible after 3 projections. To avoid this problem, each attenuation profile is subjected to amathematical high-pass filter (also referred to as"kernel") this produces overshoot and undershoot at the edges of the object.The mathematical operation is referred to as"convolution". The convolved

attenuation profiles are then added up in the image memory to produce a sharp image (CT History and Technology, 2011).

Windowing In the CT image, density values are represented as gray scale values. However, since the human eye can discern only approx. 80 gray scale values, not all possible density values can be displayed in discernible shades of gray. For this reason, the density range of diagnostic relevance is assigned the whole range of discernible gray values. This process is called windowing. To set the window, it is first defined which CT number the central gray scale value is to be assigned to. By setting the window width, it is then defined which CT numbers above and below the central gray value can still be discriminated by varying shades of gray, with black representing tissue of the lowest density and white representing tissue of the highest density (CT History and Technology, 2011).

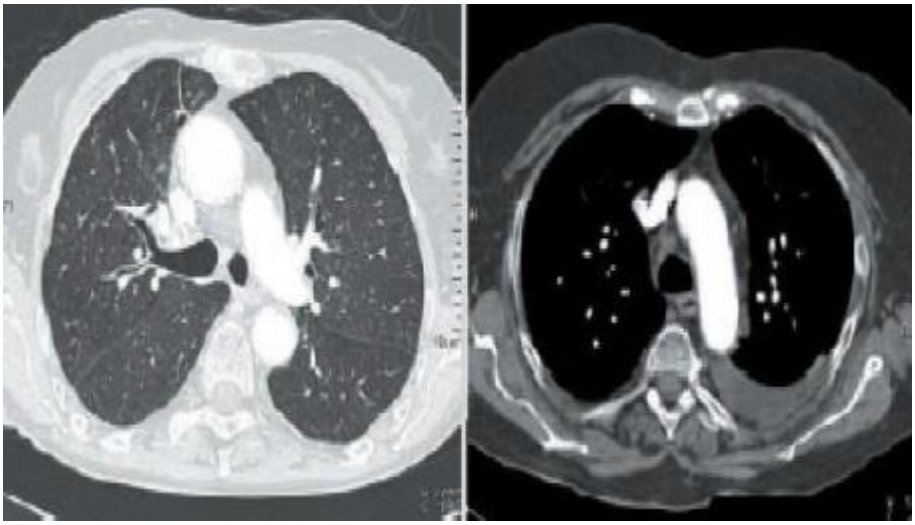

Fig 2.6 showing the long window on the left and the soft tissue window on the right

The CT image does not show these μ values directly, but the CT numbers according to Hounsfield:

CT number =1000 (μ – μwater)/ water

CT numbers are measured in HU = Hounsfield units. The CT

Number of water and air is defined as 0 HU and –1000 HU

Respectively; this scale has no limit in the positive range of values. Medical scanners typically work in a range of –1024 HU to +3071 HU (CT History and Technology, 2011).

2.1.4 Computed Radiography (CT) Generations

The terms of "generations," reflects the historical development. Current CT scanners use either third-, fourth-, or fifth generation geometries, each having their own pros and cons (Ian Acunningham and Philip F.Judy 2000).

2.1.4.1 First Generation: Parallel-Beam Geometry

Parallel-beam geometry is the simplest technically and the easiest with which to understand the important CT principles. Multiple measurements of x-ray transmission are obtained using a single highly collimated x-ray pencil beam and detector. The beam is translated in a linear motion across the patient to obtain a projection profile. The source and detector are then rotated about the patient isocenter by approximately1 degree, and another projection profile is obtained. This translate-rotate scanning motion is repeated until the source and detector have been rotated by 180 degrees.

The highly collimated beam provides excellent rejection of radiation scattered in the patient; however, the complex scanning motion results in long (approximately 5 minute) experiments but is not used in modern scanners (Ian and F.Judy 2000).

2.1.4.2 Second Generation: Fan Beam, Multiple Detectors

Scan times were reduced to approximately 30 s with the use of a fan beam of x-rays and a linear detector array. A translate-rotate scanning motion was still employed; however, a larger rotate increment could be used, which resulted in shorter scan times.

The reconstruction algorithms are slightly more complicated than those for first-generation algorithms because they must handle fan-beam projection data (Ian and F.Judy 2000).

2.1.4.3 Third Generation: Fan Beam, Rotating Detectors

Third-generation scanners were introduced in 1976. A fan beam of x-rays is rotated360 degrees around the isocenter. No translation motion is used; however, the fan beam must be wide enough to completely contain the patient. A curved detector array consisting of several hundred independent detectors is mechanically coupled to the x- ray source, and both rotate together. As a result, these rotate-only motions acquire projection data for a single image in as little as 1 s. Third-generation designs have the advantage that thin tungsten septa can be placed between each detector in the array and focused on the x-ray source to reject scattered radiation (Ian and F.Judy 2000).

2.1.4.4 Fourth Generation: Fan Beam, Fixed Detectors

In a fourth-generation scanner, the x-ray source and fan beam rotate about the isocenter, while the detector array remains stationary. The detector array consists of 600 to 4800 (depending on the manufacturer) independent detectors in a circle that completely surrounds the patient. Scan times are similar to those of third-generation scanners. The detectors are no longer coupled to the x-ray source and hence cannot make use of focused septa to reject scattered radiation. However, detectors are calibrated twice during each

rotation of the x-ray source, providing a self-calibrating system. Third-generation systems are calibrated only once every few hours. Two detector geometries are currently used for fourth-generation systems: x-ray source inside a fixed detector array and mutating detector array. the gantry components of a typical fourth-generation system using a fixed-detector array. Both third- and fourth-generation systems are commercially available, and both have been highly successful clinically. Neither can be considered an overall superior design (Ian and F.Judy 2000).

2.1.4.5 Fifth Generation: Scanning Electron Beam

Fifth-generation scanners are unique in that the x-ray source becomes an integral part of the system design. The detector array remains stationary, while a high-energy electron beams is electronically swept along a semicircular tungsten strip anode, X-rays are produced at the point where the electron beam hits the anode, resulting in a source of x-rays that rotates about the patient with no moving parts. Projection data can be acquired in approximately 50 ms, which is fast enough to image the beating heart without significant motion artifacts an alternative fifth-generation design, called (DSR) the dynamic spatial reconstructor this machine is a research prototype and is not available commercially. It consists of 14 x-ray tubes, scintillation screens, and video cameras. Volume CT images can be produced in as little as 10 ms (Ian and F.Judy 2000).

2.1.4.6 Spiral/Helical Scanning

The requirement for faster scan times, and in particular for fast multiple scans for three-dimensional imaging, has resulted in the development of spiral (helical) scanning systems. Both third- and fourth-generation systems achieve this using self-lubricating

slip-ring technology to make the electrical connections with rotating components. This removes the need for power and signal cables which would otherwise have to be rewound between scans and allows for a continuous rotating motion of the x-ray fan beam. Multiple images are acquired while the patient is translated through the gantry in a smooth continuous motion rather than stopping for each image. Projection data for multiple images covering a volume of the patient can be acquired in a single breath hold at rates of approximately one slice per second. The reconstruction algorithms are more sophisticated because they must accommodate the spiral or helical path traced by the x-ray source around the patient (Ian and F.Judy 2000).

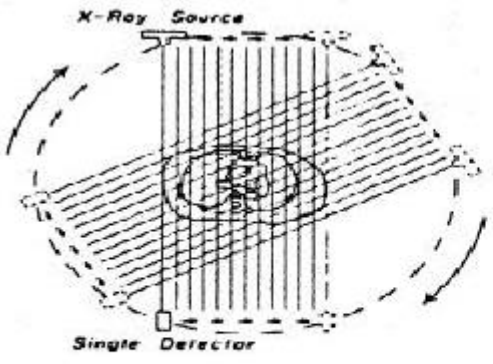

1st Generation CT Scanner
(Parallel Beam, Translate-Rotate)

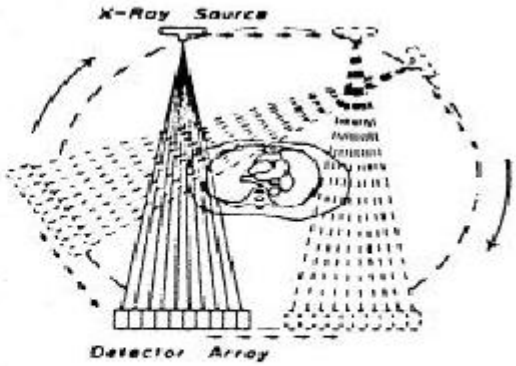

2nd Generation CT Scanner
(Fan Beam, Translate-Rotate)

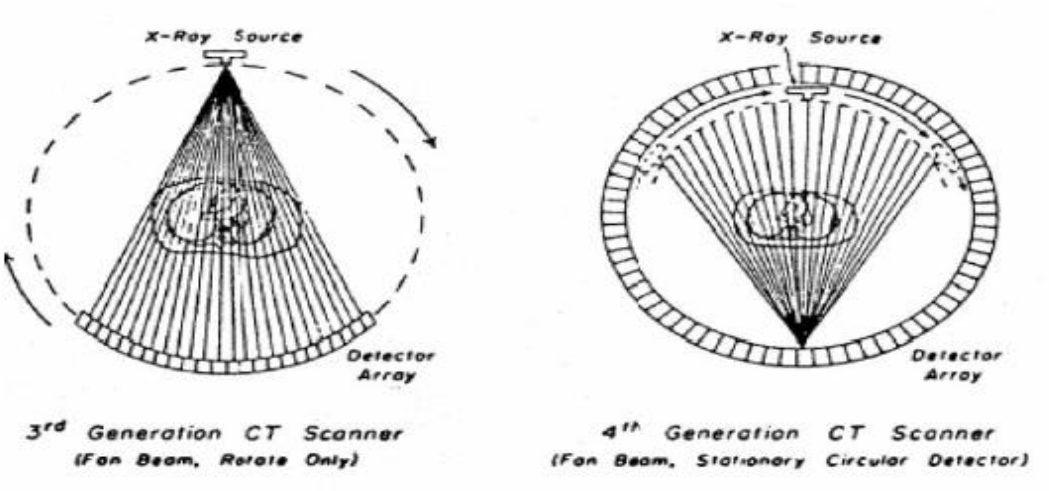

Fig 2.7 Four generations of CT scanners illustrating the parallel- and fan-beam geometries.

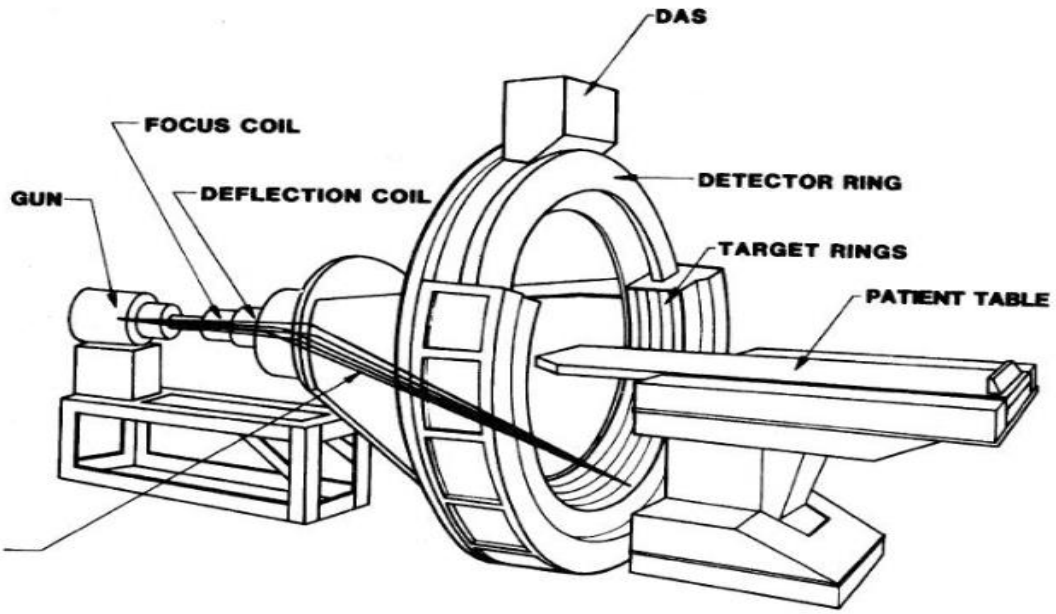

Fig 2.8 Schematic illustration of a fifth-generation ultrafast CT system Image data are acquired in as little as 50 ms, as an electron beam is swept over the strip anode electronically (Ian and F.Judy 2000).

2.2 Radiation Quantities and Unit in CT (Dosimitry)

2.2.1. CT Dosimetry and Radiation Dose

Before CT came into use, planar radiography and fluoroscopy comprised all non–nuclear medicine uses of ionizing radiation in imaging. In those types of examinations, the radiation dose to the patient maximizes where the x-ray beam enters the surface of the skin. Therefore, it has been reasonable to use radiation exposure to the entry surface (referred to as entrance skin exposure) as an indicator of radiation risk when different techniques, receptors, and x-ray machines are compared. The calculation of entrance skin exposure is straightforward, using measurements of in air ionization chamber exposure at several x-ray tube kilovoltages covering the clinical range. Such measurements are usually expressed as exposure per milliampere second (mR/mAs, or more properly today, mGy air kerma/mAs) during scanning of a CT slice, on the other hand, the x-ray beam enters from all directions at some point during the scan. It is no longer clear where (on the surface of or inside the patient) the maximum dose occurs, nor is calculation of the dose at any point in or on the patient straightforward. For example, consider 2 points, A and B, which are, respectively, near the anterior surface and at the center of a cylindrical patient. During a 360 rotation, point A receives much radiation when the x-ray tube is above the patient(nterior entry surface) . However, point A also receives some (albeit less) radiation when the tube is at every point during its rotation, even when the tube is on the opposite side of the patient. For each tube location, different amounts of radiation reach point A, depending on the depth of A(i.e., how much tissue must be penetrated) and the amount of internal scatter. By comparison, point B inside asymmetric cylindrical patient receives the same amount of radiation from all tube locations during the rotation.

Early attempts were made to estimate CT doses by using measurements of dose versus depth summed over all x-ray tube angles and positions. Though commonly used for high energy beams in radiation therapy, such dose–depth data are too sensitive to differences in x-ray spectra and tissue attenuation to be of value in CT. A different approach was needed: one based on actual measurements inside patient representative phantoms (Lee, 2007).

2.2.2CT Phantoms, Thermoluminescent Dosimeters (TLDs) and CT Dose Profiles

During development of CT dosimetry procedures, 2 standard CT dosimetry phantoms were adopted by the Food and Drug Administration and still are used today(Fig. 2.8) a 32- cm-diameter cylindrical acrylic phantom to represent an adult abdomen, and a 16-cm-diameter version to represent an adult head or small pediatric bodies(1) both are 15 cm thick insertion of dosimeters. The holes are at the center of the phantom and at a 1-cm depth at the 3-, 6-, 9-, and 12-o'clock positions (referred to as the peripheral sites) some models have holes at other locations at well (Lee, 2007).

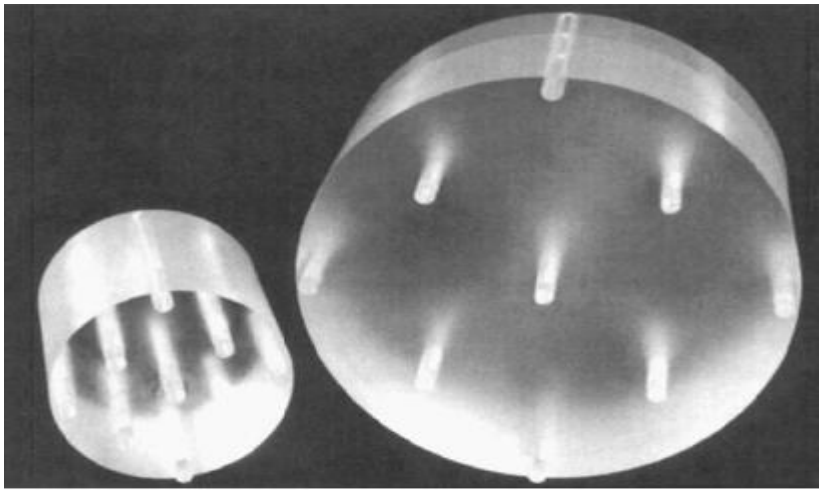

Fig 2.9 Standard CT dosimetry phantoms consist ocylindric acrylic phantoms with holes for dosimeter insertion at various locations.

A first step is to understand the nature of the radiation inside the phantom and to investigate the shape of the radiation beam in the z-direction. The z-direction x-ray beam size (the ‘‘beam width’’) is typically 10 mm or less (usually equivalent to the slice thickness). Because of practical difficulties in using ionization chambers, which were typically larger than the widths of the beams to be measured, TLDs were used for these investigations (1,2). Each TLD is a small crystal (most commonly lithium fluoride) measuring 3 mm square by 1 mm thick. Special TLD inserts were designed to hold several TLDs, allowing closely spaced x-ray dose measurements within the x-ray beam and more widely spaced measurements outside the beam (Fig. 2.9) The covered insert would be placed into a phantom hole, and a single scan would be performed with the insert centered in the slice (special alignment inserts were scanned to accurately locate the center of the slice before scanning the TLDs). The exposed TLDs were then read, and the radiation dose for each TLD was plotted against its z-axis position (Lee, 2007).

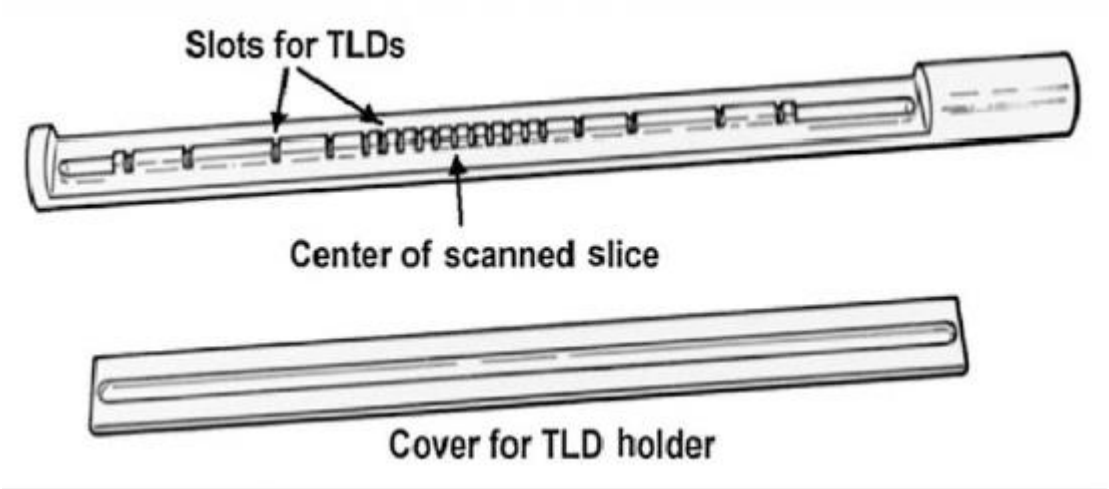

Fig 2.10 Phantom insert to hold TLDs used to measure dose profiles. TLDs are close together within x-ray primary beam and are farther apart to measure profile tails.

The conclusion is that each slice of tissue receives radiation not only when that slice is scanned but also when adjacent slices are scanned. The exact amounts of additional dose received by a slice from other slices in a series depend on several factors, including scanner geometry, collimator design, slice spacing, and the position of the slice within the series of slices. Axial (nonhelical) examinations generally consist of more than 10 slices with constant spacing. The spacing is usually equal to the slice thickness, in which case the slices are said to be contiguous. Figure 2.10 provides an example of the cumulative dose from a series of contiguous slices. The average cumulative dose to the central slices from such a series of slices with constant spacing is referred to as the multiple-slice average dose (MSAD). The MSAD may be 1.25–1.4 times the single slice dose, depending on the factors described above. The cumulative dose to the end slices is somewhat lower than that to the central slices because of a lack of contribution from the one side (Lee, 2007).

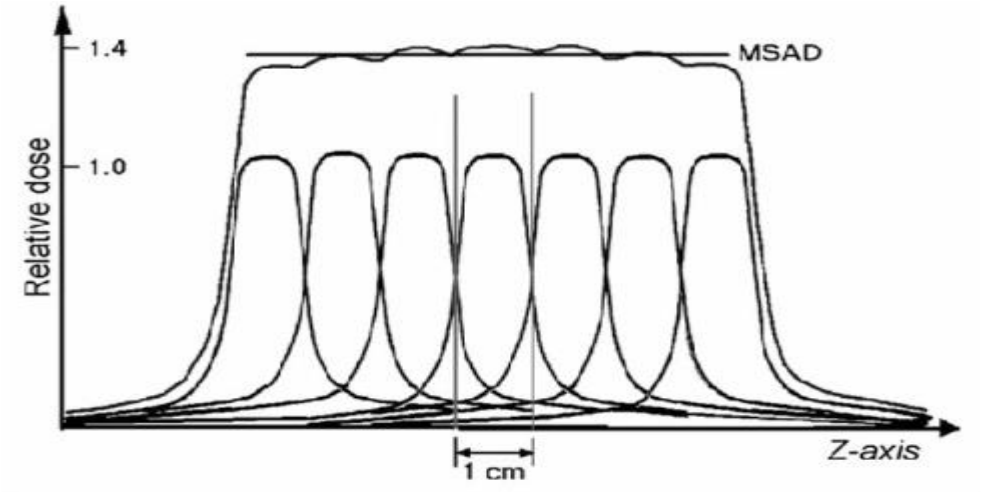

Fig 2.11 Cumulative dose from a series of contiguous slices is known as multislice average dose (MSAD)

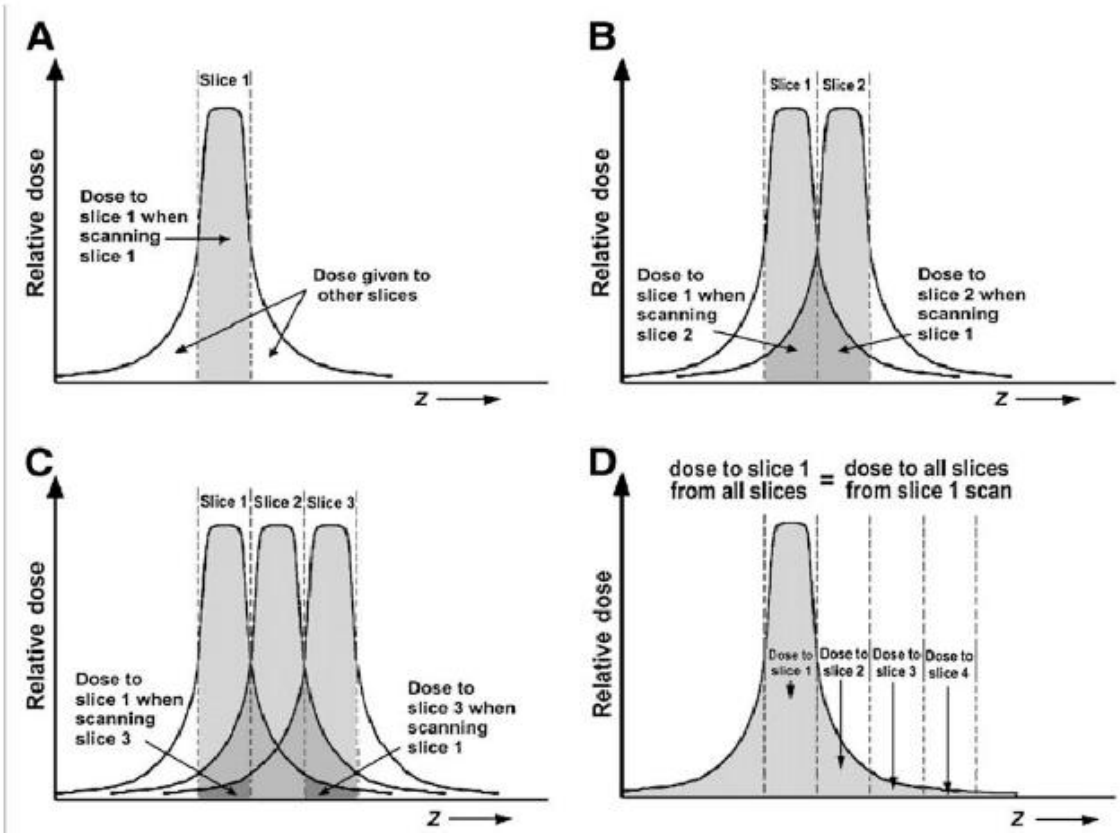

Fig 2.12 total area under dose profile, which is measured using long ionization Chamber Although informative, routine dose-profile measurements with TLDs are not clinically practical: The measurements are highly time- and labor-intensive, demand careful handling and calibration techniques, and require specialized equipment. Other methods have been used but either also were time- and labor-intensive (film-based techniques) or used devices that were not commercially available (3,4) A practical procedure was needed, and one was soon developed that directly measures a value closely related to MSAD and requires only straightforward ionization chamber measurements geometric argument diagrammed in Figure 2.11.

.

Figure 2.11 A illustrates a single-slice profile when a slice is scanned (which we denote slice 1) the shaded region represents the dose that the tissue of slice 1 receives when slice 1 is actually scanned. As noted, however, the tails of the dose profile also deposit some of the dose in adjacent slices of tissue. Now, suppose we scan a contiguous slice (slice 2) (Fig 2.12B). The darker shaded region to the right of slice 1 represents the dose that the scan of slice 1 gives to the tissue of slice 2. Note from symmetry that this dose equals that received by slice 1 when we scan slice 2. We restate this important relationship as follows: The dose that the scanning of slice 1 gives to slice 2 equals the dose that slice 1 gets from the scanning of slice 2. Continuing in this manner, we scan a third contiguous slice (Fig.2.12C). As before, the darkest shaded region to the right represents the dose deposited in slice 3 when slice 1 is scanned, which equals the dose that the scanning of slice 3 gives to slice 1. That is, the dose that the scanning of slice 1 gives to slice 3 equals the dose that slice 1 gets from the scanning of slice 3 (Lee, 2007).

By iterating in this fashion for all slices on both sides of slice 1, we arrive at the following conclusion: Dose that scanning of slice 1 gives to all slices = dose that slice 1 gets from scanning of all slices. Eq (2.1) now, consider that the dose given by slice 1 to all slices is just the total dose (i.e., the total area) underneath the single-slice dose profile of Figure 2.11 a (redrawn in Fig. 2.11 D to emphasize the entire dose under the curve). Conceptually, it is easy to measure the total dose under the profile: Use an ionization chamber sufficiently long to intercept all doses in the tails of the profile (5, 6). A commercially available CT ionization chamber 100 mm in active length is shown in Figure 2.12 (whether 100 mm is actually long enough to intercept the full profile is discussed in Appendix A). The chamber is inserted into one of the phantom holes and

centered in the hole with respect to the z-direction thickness of the phantom, and a single scan is obtained around the center of the phantom. An appropriate f-factor (usually 0.87) and calibration factor are applied to the reading, which is then multiplied by the chamber length and divided by the slice thickness (Lee, 2007).

Although a chamber measurement is used to determine the left side of Equation 1, we interpret the result as the right side: that is, as the dose a slice gets from the scanning of all contiguous slices in the series. Such a measurement is called a CT dose index (CTDI). The complete formula, using a chamber of length L, a 0.87 f-factor, and a slice of thickness T, is as follows:

$CTDI_L$ (in rads or centigrays) = chamber reading (in roentgens) *calibration factor*0.87*L/T Eq (2.1)

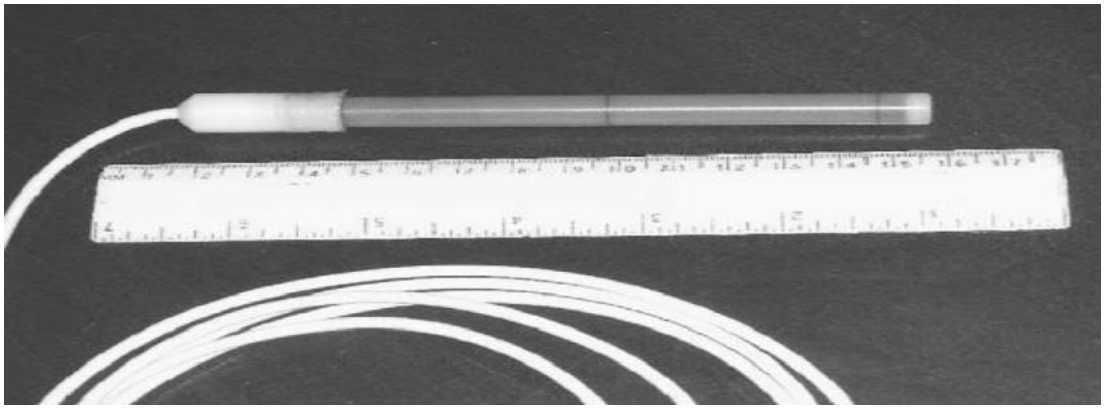

Fig 2.13 Example of 100-mm-long CT ionization chamber for measuring CTDI.

A CTDI obtained using a 100-mm chamber (the most commonly used type) is referred to as a CTDI100. Equation 2.2 is generalized for multislice CT (to be discussed in the third article of this series) by replacing T in the denominator with N ·T, where N is the number of simultaneously acquired slices of thickness T (n 5 1 for single-slice CT). Physically, N · T is the total z-direction beam width irradiating the N simultaneous slices. Applying the

factor L/T (or L/[N · T] for multislice CT) in Equation 2 is physically equivalent to assuming that the entire radiation dose intercepted by the full chamber length L was actually deposited within the thickness T of the scanned slice. We reiterate the meaning of CTDI: It is the dose (to the phantom location at which it is measured) from a complete series of contiguous slices. When this definition is compared with the definition of MSAD, it seems that CTDI and MSAD are equivalent; in fact, the only practical difference is the length of the dose profile included. Other versions of CTDI (e.g., CTDIideal and CTDIregulatory) also differ only in the length of the dose profile included. These differences are discussed in Appendix A. For our purposes, we will refer to a CTDI measured over a 100-mm profile length (CTDI100), because that is the one most commonly measured (Lee, 2007).

In general, CTDIs measured at different locations and depths in a dosimetry phantom will differ. Typical CTDIs measured at 120 kVp on a single-slice CT scan of the head and body phantoms with 5-mm collimation (5-mm slice thickness) using clinical technique. Doses for the 4 peripheral (1-cm-deep) holes are nearly uniform, as might be expected from the symmetry of a 360_ scan. The CTDI measured at the 6-o'clock position in the body phantom is often somewhat lower because of table attenuation. The CTDI at the center of the head phantom is nearly the same as that at the periphery, whereas the central CTDI in the body phantom is more than half the peripheral CTDI. A high peak kilovoltage (120) and symmetric (360) scans apparently yield doses that vary with depth only moderately in the body phantom and hardly at all in the head phantom. This somewhat counterintuitive result is due to offsetting effects: The dose from primary radiation is higher at the periphery in both cases, but the dose from scatter increases

significantly toward the center. Because the long-ionization chamber measurement includes the tails of the dose profile (which are mostly scatter) , CTDIs automatically include both primary and scatter contributions to dose (Lee, 2007).

In light of the slight-to-moderate variation in CTDI with depth, it is reasonable to ask if there is an average CTDI in the phantom that can be used as a single-number indicator of radiation dose to the patient. A commonly used such indicator is weighted CTDI ($CTDI_w$):

$$CTDIW = (2/3) * CTDIperiphery + (1/3) * CTDIcenter \quad \text{Eq (2.2)}$$

The CTDI measured at the 12-o'clock position is usually used for CTDI periphery. CTDIW values for the head and body measurement are 4.3 and 1.8 cGy, respectively. CTDIW, or a related indicator derived from it called CTDI volume, is often displayed on the CT operator's console during setting of the scan parameters (Lee, 2007).

2.2.3 CTDI for Noncontiguous Slices and CTDI for Helical Scans

The CTDI defined above and in Appendix A assumes procedures consisting of contiguous slices: that is, slice spacing I equals slice thickness T (or N · T in the case of multislice CT). This is normally the case for axial scans. For helical CT, the parameter analogous to slice spacing is table movement per rotation, which is included in helical pitch, P. Pitch is defined as table movement per rotation I divided by slice thickness T (or more generally as I divided by N · T for multislice CT)

$$P = I/[N*T] \quad \text{Eq (2.3)}$$

Because helical scans with P equal to 1 are essentially equivalent to axial scans with contiguous slices, CTDIs for such scans are about the same as for contiguous-slice axial scans using equivalent technique (equivalent peak kilovoltages, amperages, scan times,

and slice thicknesses). However, helical CT commonly uses pitches greater than 1(corresponding to wider spacing between x-ray beams of adjacent rotations) and, in multislice CT, pitches less than 1 (narrower spacing with more overlap of x-ray beams from consecutive rotations) (Lee, 2007).

To account for the effect of pitch on helical dose, and to account for axial scan doses when slice spacing I differs from slice thickness T (or N · T), the indicator CTDI volume is introduced:

$$\text{CTDI volume} = \text{CTDIW} * [N*T]/I$$

$$= \text{CTDIW} /P \qquad \text{Eq (2.4)}$$

For example, if CTDIw for a helical scan with P equal to 1 is 3 cGy, then the CTDI for the same scan protocol but with P equal to 1.5 would be 3/1.5, or 2 cGy. In effect, CTDI volume spreads the dose corresponding to CTDIw over a longer (P > 1) or Shorter (P < 1) z-axis length of tissue (Lee, 2007).

2.2.4 Dose–Length Products and Effective Dose

A sensible concern about CT radiation dose and risk regards the amount and type of anatomy irradiated. To understand the concern about the amount of irradiated anatomy, consider the following scenario: Mr. Jones undergoes a CT procedure consisting of 20 contiguous slices 5 mm thick (or equivalently, a helical scan 100 mm long with a pitch of 1). Mr. Smith undergoes a scan that is identical except for the number of slices—40 rather than 20 (or an equivalent 200-mm helical scan with a pitch of 1). In each case, the CTDIw measured in the body phantom will be the same (e.g., 3 cGy). Conceptually, however, we believe that Mr. Smith is subjected to greater radiation risk than Mr. Jones, because his radiation burden is double that of Mr. Jones (twice as much tissue received

the 3-cGy radiation dose). CTDI in any form is an estimate of average radiation dose only in the irradiated volume. Risk from ionizing radiation, however, is more closely related to the total amount of the radiation dose (i.e., energy) deposited in the patient. Clearly, Mr. Smith received more total deposited energy than did Mr. Jones. One indicator that is proportional to total deposited energy is the dose–length product, defined as follows:

$$\text{Dose – length product} = L * \text{CTDI volume} \qquad \text{Eq (2.5)}$$

where L is the total z-direction length of the examination. Some CT scanners display dose–length product along with CTDI for each scan. Although proportional to total deposited energy, dose–length product is not in itself an appropriate risk indicator, because dose–length product takes no account of the radiosensitivity of the irradiated tissues. For that purpose, the concept of effective dose (DE) has been introduced. DE is defined as the radiation dose that, if received by the entire body, provides the same radiation risk (i.e, of cancer) as does the higher dose received by the limited part of the body actually exposed (i.e, the scanned volume). Formally, the calculation of DE is complicated: we must estimate the doses deposited in each type of organ and tissue, which then are weighted according to radio sensitivity and summed. The amount of anatomy irradiated and the weighting factors for the tissues involved dramatically affect the resulting DE. The American College of Radiology, as part of its CT accreditation program, uses head and body CTDIw measurements to estimate the effective dose for routine head and abdomen examinations. For head scans, the American College of Radiology assumes a 17.5-cm total scan length and an overall tissue weighting factor of 0.0023. For the abdomen, the scan length and weighting factor are 25 cm and 0.015, respectively. Using the CTDIw values calculated and assuming contiguous slices (or a

pitch of 1), DE for the head and abdomen scans are estimated to be 0.17 and 0.68 cGy, respectively. Although the CTDIw for the head is much higher than that for the body, the abdominal DE is much Higher (4 times so) than the head DE, because the head scan irradiates a lesser amount of less radiosensitive tissue (neural tissue and bone) (Lee, 2007).

2.2.5 Scanner Design Factors Affecting CT Radiation Dose

Both scanner design factors and clinical protocol factors affect radiation dose to the patient. Some design factors that affect the radiation dose required to achieve a particular image quality have been previously discussed. Those are the factors that determine dose efficiency. The ability of a scanner to visualize low-contrast structures is inherently limited by image noise (quantum mottle). For any given radiation dose, maximum sensitivity requires capturing and using as many primary x-rays exiting the patient as possible. Dose efficiency, defined as the fraction of primary x-rays exiting the patient that contribute to the image, has 2 components: geometric efficiency (fraction of transmitted x-rays interacting with active detector areas) and absorption efficiency (fraction of actually-captured x-rays interacting with active detector areas). Geometric efficiency is reduced if some x-rays are absorbed before detection (e.g., in the detector housing) or if some x-rays do not enter active detector areas (e.g., by passing between detectors or striking inactive dividers between individual detectors). Absorption efficiency is reduced if some x-rays that enter the detectors are not absorbed (Lee, 2007).

Geometric efficiency for modern third-generation single slice scanners is relatively High (~80%), with loss being due primarily to dead spaces between detector elements. Geometric efficiency is reduced in multislice CT relative to single-slice CT, because the

separations between detector elements in the z-direction create more dead space and because more of the z-direction beam penumbra must be discarded (dose issues in multislice CT will be discussed in the third article of this series). Modern scanners generally use solid-state detectors, with absorption efficiency on the order of 99%. Other design factors that may affect radiation dose include the distance of the x-ray tube from the isocenter (and thus from the patient), the design of the prepatient x-ray beam collimator, and the design of the bowtie filter and any other beam filtration (Lee, 2007).

2.2.6 Clinical Scanning Factors Affecting CT Radiation Dose

Radiation dose depends on tube current (amperage), slice scan time, and tube peak kilovoltage. As in radiography, tube current and slice scan time are taken together as mAs in relation to radiation dose and image quality. Increasing the mAs (by increasing tube current or slice scan time) increases the dose proportionally: 300 mAs deliver twice the dose of 150 mAs. Thus, CT radiation dose is often expressed as dose per mAs (or per 100 mAs). Increasing peak kilovoltage (with all else held constant) also increases radiation dose, because the beam carries more energy. However, increasing peak kilovoltage significantly increases the intensity of the x-rays penetrating the patient to reach the detectors. Therefore, significantly lower mAs are needed to achieve similar image quality. Consequently, a higher peak kilovoltage does not necessarily mean an increased patient dose and, in fact, may allow the dose to be reduced. CT, slice thickness, slice spacing, and helical pitch may affect dose as well. In single-slice CT with well-designed collimators, dose (as indicated by CTDI) is relatively independent of slice thickness for contiguous slices. Of course, the total length of the area scanned, as well as slice spacing, will determine how much total energy is deposited in the patient. For the same

techniques, doses for helical scans with a pitch of 1.0 are equivalent to axial scans with contiguous slices. Pitches greater or less than 1 again affect CTDI values proportionally. A relatively recent innovation allowing dose reduction in many cases is mA modulation. Before mA modulation came into use, a single mA value was specified manufacturer recommendation) attenuation could change considerably along the scan length (e.g., compare attenuation through the thorax with that through the abdomen for a scan covering both areas). e.g., compare attenuation through the thorax with that through the abdomen for a scan covering both areas (and doses) for some slices, and a perhaps insufficient dose (and reduced image quality) for other slices. Using information from an initial scout view (a low-dose digital radiograph formed from a linear scan as the table moves through the gantry, with the x-ray tube stationary at, for example, 0 or 90), the scan mA value is individually adjusted, depending on z-position, for each tube rotation. An enhanced version of mA bmodulation available on some scanners allows a mA adjustment not only for each rotation (z-position) but also as a function of angle during each rotation. Angle dependent modulation is particularly valuable for anatomic regions in which a patient's anteroposterior and lateral thicknesses are quite different (e.g., the pelvis). In such cases, the preselected mA value is often insufficient to provide adequate x-ray intensity at the detectors for lateral angles or may provide excessive intensity at the detectors for anteroposterior / posteroanterior angles. Angular mA modulation optimizes mA selection for each angle to provide the least radiation dose for the required level of image quality (Lee, 2007).

Section Two

2.3 Previous Studies

In a Multi-slice helical CT: Scan and reconstruction study by Hui Hu (1998) show that a multi-slice CT scanner refers to a special CT system equipped with a multiple-row detector array to simultaneously collect data at different slice locations. The multi-slice CT scanner has the capability of rapidly scanning large longitudinal ~z! volume with high z-axis resolution. It also presents new challenges and new characteristics. In this paper, we study the scan and reconstruction principles of the multi-slice helical CT in general and the 4-slice helical CT in particular. The multi- slice helical computed tomography consists of the following three key components: the preferred helical pitches for efficient z sampling in data collection and better artifact control; the new helical interpolation algorithms to correct for fast simultaneous patient translation; and the z-filtering reconstruction for providing multiple tradeoffs of the slice thickness, image noise and artifacts to suit for different application requirements. The concept of the preferred helical pitch is discussed with a newly proposed z sampling analysis. New helical reconstruction algorithms and z- filtering reconstruction are developed for multi-slice CT in general. Furthermore, the theoretical models of slice profile and image noise are established for multi-slice helical CT. For 4-slice helical CT in particular, preferred helical pitches are discussed. Special reconstruction algorithms are developed. Slice profiles, image noises, and artifacts of 4-slice helical CT are studied and compared with single slice helical CT. The results show that the slice profile, image artifacts, and noise exhibit performance peaks or valleys at certain helical pitches in the multi-slice CT, whereas in the single- slice CT the image noise remains unchanged and the slice profile

and image artifacts steadily deteriorate with helical pitch. The study indicates that the 4-slice helical CT can provide equivalent image quality at 2 to 3 times the volume coverage speed of the single slice helical CT .in convolution The scan and reconstruction principles of multi-slice helical CT have been presented. They include the preferred helical pitch; the helical interpolation algorithms; and the z-filtering reconstruction. The concept of the preferred helical pitch has been discussed in general with a newly proposed z sampling analysis. The helical interpolation algorithms and the z-filtering reconstructions have been developed for multi-slice CT. The theoretical models of slice profile and noise have been established for multi-slice helical CT. For the 4-slice helical CT in particular, preferred helical pitches have been selected. Special helical interpolation algorithms have been developed. Image quality of the 4slice helical CT have been studied and compared with single slice helical CT. The results show that the slice profile, image artifacts, and noise exhibit performance peaks or valleys at certain helical pitches in multi-slice CT, whereas in single slice CT the image noise remains unchanged and the slice profile and image artifacts steadily deteriorate with increasing helical pitch. The study indicates that the 4-slice helical CT can provide equivalent image quality at 2 to 3 times the volume coverage speed of the single slice helical CT.

A comparative study of thoracic radiation doses from 64-slice cardiac CT a study made by E L Nickoloff, and P O Alderson (2006) indicate that measure radiation doses for 64-slice cardiac CT angiography studies and to study the dose-savings features of these CT scanners. This was done using various phantoms. These radiation doses were compared with those from typical helical body CT scans, fluoroscopy cardiac catheterization studies and mammography examinations. Radiation measurements were made with a CT

ionization detector and a solid state dosimeter. A GE 64-slice Light speed VCT and a Siemens Somatom Sensation 64 CT were used to scan a standard 32 cm acrylic phantom and an anthropomorphic phantom. Data were collected in axial and various gated cardiac helical modes. Organ doses and the effective doses were calculated from the measurements. In gated CT cardiac mode with the 32 cm acrylic phantom, the measured radiation doses per study were generally three to seven times greater than those from typical body helical CT examinations; the range depended upon selectable scan parameters. With the nanatomical phantom, the surface doses in the anteroposterior (AP) plane were typically 20–60% higher than those measured using the 32 cm phantom. The lateral surface doses were 24% to +15%. These results can be attributed to the shorter AP dimension and the air in the lungs. The CT skin entrance radiation doses were 80–90% less than diagnostic cardiac catheterization studies, and organ doses were similar. Because 64-slice cardiac gated CT uses pitches equal to 0.20– 0.27 and high mAs values, the patient radiation doses are appreciably higher than in routine body CT examinations. The female breast, which could receive a radiation dose 10–30 times that received from mammography screening, is an organ of particular concern. In conclusion Technological advances in CT imaging have opened an impressive array of diagnostic tools to physicians. The new 64-slice CT scanners performing cardiac angiography deliver significant radiation doses to the patient. In comparison with screening mammography examinations, the female breast dose from these studies is about 10–30 times greater. In comparison with a routine helical body CT study, the radiation doses are three to seven times greater. The CT skin entrance radiation doses were 80–90% less than diagnostic cardiac catheterization studies, and organ doses were similar. For both cardiac CTA and

cardiac angiography, potential risks from the relatively high radiation doses to the lungs are another major concern. It is important that the professionals who order and perform these CT examinations take prudent steps to minimize radiation exposures. Patients – especially women – should be informed about the radiation doses and receive advice about relevant risk to benefit ratios. This will allow 64-slice CT technology to be applied in the safest and most effective way possible.

Brenner, and Eric (2007) shows that the widespread use of CT represents probably the single most important advance in diagnostic radiology. However, as compared with plain-film radiography, CT involves much higher doses of radiation, resulting in a marked increase in radiation exposure in the population. The increase in CT use and in the CT-derived radiation dose in the population is occurring just as our understanding of the carcinogenic potential of low doses of x-ray radiation has improved substantially, particularly for children. This improved confidence in our understanding of the lifetime cancer risks from low doses of ionizing radiation has come about largely because of the length of follow-up of the atomic-bomb survivors -now more than 50 years - and because of the consistency of the risk estimates with those from other large-scale epidemiologic studies. These considerations suggest that the estimated risks associated with CT are not hypothetical —that is, they are not based on models or major extrapolations in dose. Rather, they are based directly on measured excess radiation-related cancer rates among adults and children who in the past were exposed to the same range of organ doses as those delivered during CT studies. In light of these considerations, and despite the fact that most diagnostic CT scans are associated with very favorable ratios of benefit to risk, there is a strong case to be made that too many CT studies are being performed in the

United States. There is a considerable literature questioning the use of CT, or the use of multiple CT scans, in a variety of contexts, including management of blunt trauma, seizures, and chronic headaches, and particularly questioning its use as a primary diagnostic tool for acute appendicitis in children. But beyond these clinical issues, a problem arises when CT scans are requested in the practice of defensive medicine, or when a CT scan, justified in itself, is repeated as the patient passes through the medical system, often simply because of a lack of communication. Tellingly, a straw poll of pediatric radiologists suggested that perhaps one third of CT studies could be replaced by alternative approaches or not performed at all. Part of the issue is that physicians often view CT studies in the same light as other radiologic procedures, even though radiation doses are typically much higher with CT than with other radiologic procedures.

A Japanese study (2010) of Radiation Exposure from CT Examinations in Japan by Yoshito Tsushima et al investigates variations in radiation exposure in CT studies among institutions and scanners. The Methods of this study is Data-sheets were sent to all 126 hospitals and randomly selected 14 (15%) of 94 clinics in Gunma prefecture which had CT scanner (s). Data for patients undergoing CT during a single month (june2008) were obtained, along with CT scan protocols for each institution surveyed. Age and sex specific patterns of CT examination, the variation in radiation exposure from CT examinations, and factors which were responsible for the variation in radiation exposure were determined. The Results was an estimated 235.4 patients per 1,000 populations undergo CT examinations each year, and 50% of the patients were scanned in two or more anatomical locations in one CT session. There was a large variation in effective dose among hospitals surveyed, particularly in lower abdominal CT (range, 2.6-19.0

mSv). CT examinations of the chest and upper abdomen contributed to approximately 73.2% of the collective dose from all CT examinations. It was estimated that in Japan, approximately 29.9 million patients undergo CT annually, and the estimated annual collective effective dose in Japan was 277.4 *103 Sv people. The annual effective dose per capita for Japan was estimated to be 2.20 mSv. There was a very large variation in radiation exposure from CT among institutions surveyed. CT examinations of the chest and upper abdomen were the predominant contributors to the collective dose.

Another study on Patient Doses for CT Examinations in Denmark by Mikkel berg (2011) shows that the current guideline was published in 2001 and concerns three main areas: mammography, conventional X-ray and computed tomography (CT). This guideline is used by the departments and clinics carrying out examinations on the approximately 125 CT-scanners in Denmark that are used for diagnostics. The current guideline does not take the increased opportunities for differentiated patient therapy into account, and the main objective of the thesis was to form the argumentative basis for the revision of the part of the current 2001 guideline that specifically relates to CT examinations. The divide was confirmed by analyzing new measurements obtained 2010/2011, by revealing a significant variance between doses within most categories. The extent and course for this variance was determined within the limits of the data. Additional relevant studies were analyzed, and the argumentative basis for the individual revisions was developed The guideline was revised into a pilot that was sent to a select number of departments, leading to a number of additional revisions that further strengthened the link between the guideline and current practice.

M. Galanski, etc, al 2005/06, pediatric CT exposure practice in the federal republic of Germany. said that. The frequency of pediatric CT examinations and the typical values of the related dose quantities (CTDIvol and DRLs) were surveyed in the ten Swiss centres performing pediatric CT. Mean values averaged over the participating centres were calculated and the corresponding DRLs were established by multiplying the mean values by 1.25. This investigation revealed that 4,000–5,000 CT examinations are carried out on children in Switzerland, with an average of 453 per centre performing pediatric CT. Significant variations of the radiation dose delivered to the pediatric population were found. An optimization process should be initiated in order to reduce this spread in dose (appropriate image quality requirements for a given indication, number of acquisition phases that are clinically relevant, etc.). A major element of the optimization process is a consensus on the DRLs that need to be used. This becomes a priority in the light of contributions such as described in a recent article published in the Lancet A set of DRL values for CT examinations of the brain, the chest and the abdomen and for the various age groups are proposed here for temporary use in pediatrics until a more extensive survey is organized to collect dose data on a large sample of patients and to establish empirical dose distributions. The frequency of pediatric CT examinations and the typical values of the related dose quantities (CTDIvol and DRLs) were surveyed in the ten Swiss centers performing pediatric CT. Mean values averaged over the participating centers were calculated and the corresponding DRLs were established by multiplying the mean values by 1.25. This investigation revealed that 4,000–5,000 CT examinations are carried out on children in Switzerland, with an average of 453 per centre performing pediatric CT. Significant variations of the radiation dose delivered to the pediatric population were

found. An optimization process should be initiated in order to reduce this spread in dose (appropriate image quality requirements for a given indication, number of acquisition phases that are clinically relevant, etc.). A major element of the optimization process is a consensus on the DRLs that need to be used. This becomes a priority in the light of contributions such as described in a recent article published in the Lancet. A set of DRL values for CT examinations of the brain, the chest and the abdomen and for the various age groups are proposed here for temporary use in pediatrics until a more extensive survey is organized to collect dose data on a large sample of patients and to establish empirical dose distributions.

The author Fracis R et al (2008), CT radiation dose in children: survey to established age-based diagnostic reference levels in Switzerland, were said; This work aimed at assessing the doses delivered in Switzerland to paediatric patients during computed tomography (CT) examinations of the brain, chest and abdomen, and at establishing diagnostic reference levels (DRLs) for various age groups. Forms were sent to the ten centers performing CT on children, addressing the demographics, the indication and the scanning parameters: number of series, kilovoltage, tube current, rotation time, reconstruction slice thickness and pitch, volume CT dose index (CTDIvol) and dose length product (DLP). Per age group, the proposed DRLs for brain, chest and abdomen are, respectively, in terms of CTDIvol: 20, 30, 40, 60 mGy; 5, 8, 10, 12 mGy; 7, 9, 13, 16 mGy; and in terms of DLP: 270, 420, 560, 1,000 mGy cm; 110, 200, 220, 460 mGy cm; 130, 300, 380, 500 mGy cm. An optimization process should be initiated to reduce the spread in dose recorded in this study. A major element of this process should be the use of DRLs. The frequency of pediatrics CT examinations and the typical values of the related dose

quantities (CTDIvol and DRLs) were surveyed in the ten Swiss centers performing pediatrics CT. Mean values averaged over the participating centers were calculated and the corresponding DRLs were established by multiplying the mean values by 1.25. This investigation revealed that 4,000–5,000 CT examinations are carried out on children in Switzerland, with an average of 453 per centre performing pediatric CT. Significant variations of the radiation dose delivered to the pediatric population were found. An optimization process should be initiated in order to reduce this spread in dose (appropriate image quality requirements for a given indication, number of acquisition phases that are clinically relevant, etc.). A major element of the optimization process is a consensus on the DRLs that need to be used. This becomes a priority in the light of contributions such as described in a recent article published in the Lancet. A set of DRL values for CT examinations of the brain, the chest and the abdomen and for the various age groups are proposed here for temporary use in pediatrics until a more extensive survey is organized to collect dose data on a large sample of patients and to establish empirical dose distributions.

Buls et al (2010) studied about CT pediatrics doses in Belgium: a multi-centre they found that This multi-centre study evaluated CT exposure of children in Belgium by investigating radiological practice and patient doses for five common CT examinations over five age ranges. The study was conducted by a consortium of Belgian research groups of both medical physicists and radiologists that are involved in pediatric CT. The study was initiated in 2007 and data was collected and processed until 2009. After a nation-wide mailing, 18 hospitals representing radiology centers participated in the study. The hospitals (7 university hospitals and 11 general hospitals) were dispersed over the

whole Belgian region. In local audits by group of medical physics experts, dosimetry measurements were performed by determining the standard CT dose descriptors for each particular CT examination protocol that was used for children. The applied technical scan parameters by the CT users were obtained and reviewed, and radiological image quality was assessed by pediatric radiologists. The collected data were compared to results from other European nation-wide studies.

The author Tilo Niemann et al (2015) studies the increasing absolute number of pediatric CT scans raises concern about the safety and efficacy and the effects of consecutive diagnostic ionizing radiation. To demonstrate a method to evaluate the lifetime attributable risk of cancer incidence/mortality due to a single low-dose helical chest CT in a two-year patient cohort. Materials and methods A two-year cohort of 522 pediatric helical chest CT scans acquired using a dedicated low-dose protocol were analyzed retrospectively. Patient-specific estimations of radiation doses were modelled using three different mathematical phantoms. Per-organ attributable cancer risk was then estimated using epidemiological models. Additional comparison was provided for naturally occurring risks. Results Total lifetime attributable risk of cancer incidence remains low for all age and sex categories, being highest in female neonates (0.34%). Summation of all cancer sites analyzed raised the relative lifetime attributable risk of organ cancer incidence up to 3.6% in female neonates and 2.1% in male neonates. Conclusion Using dedicated scan protocols, total lifetime attributable risk of cancer incidence and mortality for chest CT.

Author author Jenia Vassileva et al (2013) in a survey procedures and protocols in pediatrics computed tomography (CT) in 40 less resourced countries. Methods Under a

project of the International Atomic Energy Agency, 146 CT facilities in 40 countries of Africa, Asia, Europe and Latin America responded to an electronic survey of CT technology, exposure parameters, CT protocols and doses. Results Modern MDCTsystems are available in 77 % of the facilities surveyed with dedicated pediatrics CT protocols available in 94 %. However, protocols for some age groups were unavailable in around 50 % of the facilities surveyed. Indication-based protocols were used in 57 % of facilities. Estimates of radiation dose using CTDI or DLP from standard CT protocols demonstrated wide variation up to a factor of 100. CTDIvol values for the head and chest were between two and five times those for an adult at some sites. Sedation and use of shielding were frequently reported; immobilization was not. Records of exposure factors were kept at 49 % of sites. Conclusion There is significant potential for improvement in CT practice and protocol use for children in less resourced countries. Dose estimates for young children varied widely. This survey provides critical baseline data for ongoing quality improvement efforts by the IAEA.

Chapter Three

Materials and Methods

3.1 Materials and Methods:

The data of this study were collected from Alya hospital, Ibn Alhitham specialist, Alzytouna hospital and Modern center. Data of the technical parameters used in CT procedures was taken during June 2016 –June 2018.

3.2 CT machines:

Table 3.1 shows CT machine data

Hospital	***Manufacturer***	***Model***	***Detected Type***
Alya Hospital	Toshiba	Adelion	64
Ibn Alhitham Hospital	Toshiba		4 slice
Alzytouna Hospital	Toshiba	Agullion	64 slice
Modern Center	GE	Optima 520	16 slice

All quality control tests were carried out for the machines by experts from Sudan Atomic Energy Commission (SAEC) prior to any data collection, The entire hospital was passed successfully the extensive quality control tests. All quality control tests were performed to the machine prior any data collection. All data were within acceptable ranges.

3.3 Patient data:

A total of 336_patients with different CT examinations were referred to Alya hospital, Ibn Alhitham specialist, Alzytouna hospital and Modern center. in the period of study. All the patients were performed using departments' protocols with Multi slice CT (MSCT) 8, 16, 64 slice.

This study was designed to evaluate the patient doses and the radiation related factor, the collected data included, sex, and age, tube potential, tube current–time product settings, pitch, slice thickness and total slice number, in addition, I also recorded all scanning parameters, as well as the CT Dose Index volume (in milli sievert) and dose-length product (in milli sievert-centimeters). All these factors have a direct influence on radiation dose. The collection of the patient exposure parameters was done using patient dose survey forms prepared for collection of patient exposure- related parameters.

3.4 CT dose measurements:

Radiation dose indicators $CTDI_{vol}$ and DLP can be obtained from a dose summary page, which includes information about the CT exam. $CTDI_{vol}$ does allow the comparison of scan protocols or scanners and is useful for obtaining benchmark data to compare techniques, but it's not so good for estimating patient dose.

DLP, an indicator of the dose imparted to the patient, is calculated by multiplying $CTDI_{vol}$ times the scan length. In addition to being affected by the issues associated with $CTDI_{vol}$, DLP can be problematic in a limited scan range. For the sake of simplicity, the CTDI100, air will henceforth be abbreviated as CTDIair.

3.5 Imaging techniques

The data were collected for patient during the routine CT imaging protocols in these departments. No modifications were made for dose optimisation in this stage of the research. In general the imaging protocols were based on the following steps:

1. Have a technologist meet with the patient before the exam to confirm that symptoms match the indications for the CT exam.
2. Choose a specific exam protocol which addresses the clinical question while minimizing dose.
3. Center the patient carefully. Asymmetric positioning can result in decreased image quality and an increase in patient dose.

3.6 Calculation of Effective dose

CT scanners record the radiation exposure as a DLP in mGy.cm. and by Multiply this by Conversion Factor (CF) to convert it to effective dose in mSv.

3.7 Cancer risk estimation:

The risk (RT) of developing cancer in a particular organ (T) following CT exam after irradiation was estimated by multiplying the mean organ equivalent (H_T) dose with the risk coefficient (f_T) obtained from ICRP [ICRP 2006, ICRP 2007]. The overall lifetime mortality risk per procedure resulting from cancer/heritable was determined by multiplying the effective dose (E) by the risk factor (f). The risk of genetic effects in future generations was obtained by multiplying the mean dose to the gonads by the risk factor [ICRP 2006, ICRP 2007].

$$R = E.f = \sum R_T \quad \text{Equation (3.1)}$$

Table 3.2 Radiation risk for patient and workers:

Exposed population	Cancer		Heritable effects		Total	
	ICRP 103(2)	ICRP 60 (19)	ICRP 103	ICRP 60	ICRP 103	ICRP 60
Whole population *	5.5	6.0	0.2	1.3	6.0	7.3
Adults workers**	4.1	4.8	0.1	0.8	4.0	5.6
Children	NA	13	0.08	0.1	NA	NA

*Age between 0-90 years old ** Adults workers aged 18-64

It is important to note that alternative methods and conversion coefficient exist to calculate the effective dose. This estimate only and can differ from other estimates by as much as a factor of 2. This estimate is not the dose for any given individual, but rather, for a standardized anthropomorphic phantom, representative of the "whole body equivalent" radiation detriment (risk) associated with the "partial body" CT examination. These values can be used to optimize protocols, and as a broad indication of the relative risk of the CT examination compared to background radiation or examinations from other modalities.

Chapter Four

Results

The amount of radiation dose a patient receives from a CT scan depends upon two key factors, the design of the scanner and also on the way that the scanner is used. The designs of single slice and multi-slice scanners are similar in most aspects that affect radiation dose, but multi-slice scanning can potentially result in higher radiation risk to the patient due to increased capabilities allowing long scan lengths at high tube currents.

It is well known fact that CT imaging is the largest source of medical exposure nowadays. As the growth in CT utilization increased, particularly in pediatric patients, and as concern about the population dose from CT began to be expressed in the scientific literature and lay press, it became clear that the responsible use of CT required an adjustment of technique factors on the basis of patient size (attenuation characteristics). In response to these concerns, the radiology community (radiologists, medical physicists, and manufacturers) implemented CT dose management procedures that correspond to the principle of ALARA (as low as reasonably achievable). In this study, a total of 336 patients were examined in four Hospital in Khartoum over 2 years (Alyaa , Alzytouna , Ibn alhytham , Modern Center).

Table 4.1 show the number of both adult patients male- female:

Gender	Frequency	Percent
Female	118	51.1
Male	113	48.9
Total	231	100.0

Table 4.2 show statistical parameters for demographic and radiological parameters for all patients:

Variables	***Mean***	***Median***	***STD***	***Min***	***Max***
Age (year)	49	50	19.57	18	86
BMI	26.56	26.23	4.23	19.14	72.97
kV	120	120	0.00	120	120
mA	198.80	214	72.52	60	707
DLP(mGy/cm)	1640.23	1436	2339	70	26636
CTDIvol(mSv/cm)	55.15	72.2	39.81	4.02	239
Effective Dose(mSv)	12.189	8.62	11.7	0.318	79.71

Table 4.3 show statistical parameters for demographic and radiological parameters for male at all hospitals:

Variables	***Mean***	***Median***	***STD***	***Min***	***Max***
Age (year)	50.80	50	19.24	18	85
BMI	25.49	28.53	3.47	19.53	39.44
kV	120	120	0.00	120	120
mA	197.91	211	77.27	60	707
DLP(mGy/cm)	1639.35	1438	2601.64	136	26636
CTDIvol(mSv/cm)	56.1	72.2	42.42	4.05	239
Effective Dose(mSv)	12.33	9.17	11.28	0.841	55.94

Table 4.4 show statistical parameters for demographic and radiological parameters for female at all hospitals:

Variables	***Mean***	***Median***	***STD***	***Min***	***Max***
Age (year)	47.44	45.50	19.81	18	86
BMI	27.57	27.55	4.64	19.14	42.97
kV	120	120	0.00	120	120
mA	199.65	224	67.96	60	578
DLP(mGy/cm)	1582.34	1361	2069.07	70	19537
CTDIvol(mSv/cm)	54.24	71.5	37.29	4.02	143.1
Effective Dose(mSv)	13.13	9.66	12.32	0.333	79.71

Table 4.5 show statistical parameters for demographic and radiological parameters for brain exam at Alyaa Hospital:

Variables	***Mean***	***Median***	***STD***	***Min***	***Max***
Age (year)	53.46	55.5	17.62	18	86
BMI	26.64	26.49	40.05	19.81	34.68
kV	120	120	0.00	120	120
mA	122.27	125	17.3	92	193
DLP(mGy/cm)	1563.84	1541.75	431.92	151.50	2535
CTDIvol(mSv/cm)	75.18	75.4	3.13	72.20	89
Effective Dose(mSv)	3.29	3.24	0.90	0.32	5.32

Table 4.6 show statistical parameters for demographic and radiological parameters for chest exam at Alyaa Hospital:

Variables	***Mean***	***Median***	***STD***	***Min***	***Max***
Age (year)	56.52	65	20	21	85
BMI	27.76	27.82	3.93	20.72	34.41
kV	120	120	0.00	120	120
mA	174.60	170	36.64	118	250
DLP(mGy/cm)	543.17	551.2	201.76	204.9	869.30
CTDIvol(mSv/cm)	14.62	14.5	3.92	4.9	18.7
Effective Dose(mSv)	7.6	7.7	2.83	2.87	12.17

Table 4.7 show statistical parameters for demographic and radiological parameters for brain exam at Alzytouna Hospital:

Variables	***Mean***	***Median***	***STD***	***Min***	***Max***
Age (year)	50.6	52.5	23.47	18	85
BMI	24.98	24.62	3.22	20.19	32.83
kV	120	120	0.00	120	120
mA	255	255	.00	255	255
DLP(mGy/cm)	1585	1569	432.5	158	3313
CTDIvol(mSv/cm)	80.84	77	13.65	77	155
Effective Dose(mSv)	3.32	3.29	0.908	0.333	6.96

Table 4.8 show statistical parameters for demographic and radiological parameters for chest exam at Alzytouna Hospital:

Variables	***Mean***	***Median***	***STD***	***Min***	***Max***
Age (year)	45.72	45	23.27	11	85
BMI					
kV	120	120	0.00	120	120
mA	255	255	.00	255	255
DLP(mGy/cm)	1617.87	1554	467	158	3313
CTDIvol(mSv/cm)	84.72	77	28.21	77	239
Effective Dose(mSv)	22.65	21.75	6.54	2.21	46.38

Table 4.9 show statistical parameters for demographic and radiological parameters for brain exam at Ibnalhytham Hospital:

Variables	***Mean***	***Median***	***STD***	***Min***	***Max***
Age (year)	45.83	39	20.7	18	79
BMI	26.8	25.76	5.53	21.20	42.96
kV	120	120	0.00	120	120
mA	244.17	300	77.33	112	300
DLP(mGy/cm)	5006.76	5404.2	6214.02	400.3	26636
CTDIvol(mSv/cm)	107.65	143.1	43.65	21.8	154.62
Effective Dose(mSv)	10.52	11.35	13.04	0.84	55.93

Table 4.10 show statistical parameters for demographic and radiological parameters for chest exam at Ibnalhytham Hospital:

Variables	***Mean***	***Median***	***STD***	***Min***	***Max***
Age (year)	46.8	46	15.89	19	70
BMI	26.57	26.27	4.62	19.53	39.52
kV	120	120	0.00	120	120
mA	159.75	187	49.14	60	187
DLP(mGy/cm)	631.65	655	319.33	185.3	1509
CTDIvol(mSv/cm)	18.69	19.4	9.25	5.4	41
Effective Dose(mSv)	8.93	9.17	4.47	2.59	21.13

Table 4.11 show statistical parameters for demographic and radiological parameters for brain exam at Modern Center:

Variables	***Mean***	***Median***	***STD***	***Min***	***Max***
Age (year)	43.68	43.50	20.23	18	75
BMI	25.08	25.83	2.93	20.06	30.38
kV	120	120	0.00	120	120
mA	251.95	252.5	27	223	318
DLP(mGy/cm)	642.15	617.61	80.21	519.7	817.35
CTDIvol(mSv/cm)	43.59	43.26	3.83	38.88	53.79
Effective Dose(mSv)	1.35	1.29	0.17	1.09	1.72

Table 4.12 show statistical parameters for demographic and radiological parameters for chest exam at Modern Center:

Variables	***Mean***	***Median***	***STD***	***Min***	***Max***
Age (year)	47.86	45	18.33	18	75
BMI	26.92	27.92	4.09	20.76	34.92
kV	120	120	0.00	120	120
mA	132.33	83	71.64	80	300
DLP(mGy/cm)	557.65	404.29	366.07	230.5	1551.56
CTDIvol(mSv/cm)	9.84	9.57	3.92	4.02	18.56
Effective Dose(mSv)	7.81	5.66	5.13	3.22	21.72

Table 4.13 show statistical parameters for demographic and radiological parameters for all pediatric patients:

Variables	***Mean***	***Median***	***STD***	***Min***	***Max***
Age (year)	3.15	4	1.62	1	5
BMI	16.09	15.8	1.50	13.6	20.8
kV	120	120	0.00	120	120
mA	163.1	125	89.49	27	529
DLP(mGy/cm)	756.25	605	477.24	103.5	2196
CTDIvol(mSv/cm)	43.90	38.9	25.8	2.9	80.0
Effective Dose(mSv)	8	6.4	5.24	1.9	32.52

Table 4.14 show the number of both pediatric patients male- female:

Gender	Frequency	Percent
Female	41	39.0
Male	64	61.0
Total	105	100.0

Table 4.15 show statistical parameters for demographic and radiological parameters for male at all hospitals:

Variables	***Mean***	***Median***	***STD***	***Min***	***Max***
Age (year)	3.31	4	1.7	1	5
BMI	15.90	15.8	1.26	13.8	20.58
kV	120	120	0.00	120	120
mA	168.31	138	92.58	27	529
DLP(mGy/cm)	781.87	543.36	535.36	103.47	2196
CTDIvol(mSv/cm)	42.77	38.77	25.87	2.9	75.4
Effective Dose(mSv)	7.75	6	5	1.7	24.2

Table 4.16 show statistical parameters for demographic and radiological parameters for female at all hospitals:

Variables	***Mean***	***Median***	***STD***	***Min***	***Max***
Age (year)	2.9	2	1.53	1	5
BMI	16.8	15.7	1.8	13.6	20.8
kV	120	120	0.00	120	120
mA	154.8	125	84.9	38	404
DLP(mGy/cm)	716.25	621.7	371.7	187	1366
CTDIvol(mSv/cm)	45.8	36.9	25.6	2.9	80.8
Effective Dose(mSv)	8.3	6.6	5.6	1.9	32.5

Table 4.17 show statistical parameters for demographic and radiological parameters for brain exam at Alzytouna Hospital:

Variables	***Mean***	***Median***	***STD***	***Min***	***Max***
Age (year)	3.33	4	1.6	1	5
BMI	14.92	15.65	3.41	2.06	18.06
kV	120	120	0.00	120	120
mA	229.22	223.5	21.7	223.5	313.5
DLP(mGy/cm)	571	543	66.2	466.3	685.9
CTDIvol(mSv/cm)	39.3	38.9	2.5	37.5	46.1
Effective Dose(mSv)	6.3	6	0.73	5.13	7.6

Table 4.18 show statistical parameters for demographic and radiological parameters for chest exam at Alzytouna Hospital:

Variables	***Mean***	***Median***	***STD***	***Min***	***Max***
Age (year)	4	5	1.7	1	5
BMI	15.9	16.5	1.3	14	17
kV	120	120	0.00	120	120
mA	291	215	168	146	529
DLP(mGy/cm)	173	187	44.5	106	214
CTDIvol(mSv/cm)	5.8	6	3.3	3	11
Effective Dose(mSv)	4.5	4.9	1.2	2.8	5.6

Table 4.19 show statistical parameters for demographic and radiological parameters for brain exam at Alyaa Hospital:

Variables	***Mean***	***Median***	***STD***	***Min***	***Max***
Age (year)	2.8	2	1.7	1	5
BMI	15.8	15.9	1.13	13.6	17.3
kV	120	120	0.00	120	120
mA	101.4	111	29	17	125
DLP(mGy/cm)	1152.8	1306.6	469.8	22	218
CTDIvol(mSv/cm)	67.5	72.2	16.9	22.8	80.8
Effective Dose(mSv)	7.7	6.5	3.7	2	14.6

Table 4.20 show statistical parameters for demographic and radiological parameters for chest exam at Alyaa Hospital:

Variables	***Mean***	***Median***	***STD***	***Min***	***Max***
Age (year)	3.8	4.5	2	1	5
BMI	15.6	15.8	1.3	14	16.8
kV	120	120	0.00	120	120
mA	310	282.5	189	146	529
DLP(mGy/cm)	169.5	178.8	50.4	106.1	214.2
CTDIvol(mSv/cm)	4.6	4.4	1.8	3	6.2
Effective Dose(mSv)	4.2	3.7	1.7	3.1	6.4

Table 4.21 show statistical parameters for demographic and radiological parameters for brain exam at Ibnalhytham Hospital:

Variables	***Mean***	***Median***	***STD***	***Min***	***Max***
Age (year)	3	2.5	1.7	1	5
BMI	16.9	17.02	2	13.9	20.81
kV	120	120	0.00	120	120
mA	101.4	111	29.1	27	125
DLP(mGy/cm)	1152.80	1306.6	469.8	282	2196
CTDIvol(mSv/cm)	67.5	72.2	16.9	22.8	80.8
Effective Dose(mSv)	12.7	14.4	5.2	3.1	24.17

Table 4.22 show statistical parameters for demographic and radiological parameters for chest exam at Ibnalhytham Hospital:

Variables	***Mean***	***Median***	***STD***	***Min***	***Max***
Age (year)	3.6	4	1.2	2	5
BMI	15.3	15.4	1.5	13.7	16.8
kV	120	120	0.00	120	120
mA	154	150	25.1	130	180
DLP(mGy/cm)	491.2	512	187	199.6	652.2
CTDIvol(mSv/cm)	15.12	16	2.8	12	18
Effective Dose(mSv)	12.8	13.31	4.9	5.2	17

Table 4.23 show statistical parameters for demographic and radiological parameters for brain exam at Modern center:

Variables	***Mean***	***Median***	***STD***	***Min***	***Max***
Age (year)	3.33	4	1.6	1	5
BMI	9559.3	14314.3	7894.24	14.4	18055.6
kV	120	120	0.00	120	120
mA	229.22	223.5	21.17	223.5	313.5
DLP(mGy/cm)	571	544	66.21	466.3	686
CTDIvol(mSv/cm)	39.3	39.9	2.5	37.5	46
Effective Dose(mSv)	3.6	3.2	1.7	1.9	7.3

Table 4.24 show statistical parameters for demographic and radiological parameters for chest exam at Modern center:

Variables	***Mean***	***Median***	***STD***	***Min***	***Max***
Age (year)	2.7	2	1.7	1	5
BMI	17	17.31	1.73	14.7	20.6
kV	120	120	0.00	120	120
mA	85.5	80	9.4	80	100
DLP(mGy/cm)	375.18	292.2	305.11	103.6	1250.82
CTDIvol(mSv/cm)	9.24	10.04	3.3	4.02	13.7
Effective Dose(mSv)	9.7	7.52	8.4	1.9	32.5

Table 4.25 show the effective dose for brain and chest in all hospital for adult and pediatric:

	Adult		***Pediatric***	
Hospital	***Brain***	***Chest***	***Brain***	***Chest***
A ED mSv	3.29	7.6	7.7	4.2
B ED mSv	3.32	22.65	6.3	4.5
C ED mSv	10.52	8.93	12.7	12.8
D ED mSv	1.35	7.81	3.6	9.7

Table 4.26 compare the present study with diagnostic reference level and other countries (adult):

	CTDIvol (mGy)	***DLP (mGy.cm)***
Present Study 2019	54.4	1518.6
Japan 2015	85	1350
United kingdom 2013	39	544
European DRL 2013	60	1050
Australian 2013	60	1000
ICRP 2001	60	1050
Adam Lukasiewicz,et al;2014	NA	746

Table 4.27 compare the present study with diagnostic reference level and other countries (pediatric):

	CTDIvol (mGy)	***DLP (mGy.cm)***	***Effective Dose (mSv)***
Present Study 2019	54.4	1518.5	*8.01*
D. L. Miglioretti et al 2013 – USA	NA	NA	*3.5*
Ataç, et al 2015-turkey	22.95	262.75	*1.5*
Thomas KE et al 2008 – USA	3.02	46.38	*1.5*
Shrimpton PC et al 2006 – UK	NA	NA	*1.5*
Tilo Niemann et al - 2015	1.47	45	*1.93*

Chapter Five

Discussion

5.1 Discussion

The use of CT as diagnostic tool in imaging has increased over the last years, comparing it with other diagnostic techniques. Radiation exposure from CT is high thus the risk of inducing cancer from CT is relatively high and it is very important due to the rapid use of CT scanner there for reducing the radiation dose significantly important by using technique that minimizing radiation exposure (ALARA concept) and limit patient dose.

The importance of the study comes from the increased number of patient in CT investigations. It had been estimated the CT examinations are increasing yearly 10%. Radiation induced cancer is one of the main issues which attract special attention due to large number of population undergoing these investigations. The researcher assess radiation exposure from different CT scans at 4 hospital.(Alyaa Hospital , Ibn Alhaytham Hospital, Alzytouna Hospital, Modern center) for adult and pediatric. The group age in this study was in the range of (0-85) years old.

Patient dose in CT depend on the used exposure parameter (kVp, mA rotation time focal spot size, scan field of view, slice width and pitch and X-ray beam collimation on multi-slice scanners) this parameter must be selected carefully for each patient taken in to account patient age and BMI especially in pediatric patients to optimize radiation dose and reduce radiation risk.

Manufactories generally recommended tube current and time sittings for different examination for a standard size patient and the operator must decide whether , and if so , by who much, to adjust

these setting to take into account variation in patient size for digital system, such as CT scanners. Radiation exposure has been an important issue in CT since the technique was introduced three decade ago. Because CT is a major source of radiation for the population, an effort to minimize dose is critically important.

Effective dose is unit for choice in CT when the patient exposue to high radiation dose and partial exposure also it a good indicator for compression between different CT examination, since DLP and CTDIv will provide less information regarding the radiation risks.

Patient data for both male and female collected from four different hospital and centers in Khartoum which using different CT scanner modalities at four hospitals to scan chest and brain for adult patient (18-78) years old with total number of 231 adult patient. Table 4.1 present the demographic and radiographic information for patients underwent CT brain and chest examinations as mean ± standard deviation, and for the radiographic data the kV was 120 for all patients for age and body mass index was 49 ± 19.57 and 26.56 ± 4.23, for mA, DLP, CTDIvol and effective dose was 198.80 ± 72.52, 1646.23 ±2339, 55.15 ± 39.81 and 12.189 ±11.7 respectively. Comparing the demographic and radiographic information from CT brain and chest among male and female for age and BMI the age data shows the males was older than female 50.80± 19.24 years and 47.44 ±19.81 years and the body mass index data its higher for female than male 27.57±4.64, 25.49 ±3.47 . The radiographic data the mA and effective dose were higher for female 199.65± 67.96, 13.13± 12.32 for male was 197.91± 77.27, 12.33± 11.28 while the DLP and CTDIvol were higher for male 1639.35± 2601.64, 56.1± 42.42, the data for female 1582.34± 2069.07, 54.24 ±37.29 , this increasment in the effective dose due to the high BMI for female.

Table 4.3 and table 4.4 show statistical parameters for demographic and radiological parameters for male and female at all hospitals were the data presented as mean ± STD for the demographic information there is an increase in BMI, mA and effective dose for female 27.57± 4.64, 199.65± 67.96, 13.13± 12.32.as for male 25.49± 3.47, 197.91± 77.27, 12.33 ±11.28. male has the highest value for age, DLP, CTDIv 50.80 ± 19.24, 1639.35 ± 2601.64, 56.1± 42.42.as for female 47.44± 19.81, 1582.34± 2069.07, 54.24 ± 37.29 respectively.

Tables 4.5, 4.7, 5.9 and 4.11 shows the statistical parameters for demographic and radiological parameters for brain (adult) examinations as mean ± standard deviation Ibnalhytem Hospital(4 slice, 2.5 slice/ rotation) has the highest effective dose level , DLP and CTDIv 10.52 ± 13.04, 5006.70 ± 6214.04, 107.65± 43.65 respectively due to large BMI effecting CTDIv and DLP witch increased ED. Tables 4.6,4.8, 4.10 and 4.12 shows the statistical parameters for demographic and radiological parameters for chest (adult) examinations as mean ± standard deviation Alzytouna Hospital(64 slice , 10 slice/ rotation) has the highest effective dose level , DLP and CTDIv 22.65± 6.54, 1617.87± 4.67, 84.72 ±28.21 due to high mA used in this examination.

Table 4.13 shows the demographic data and radiographic information for all patients (pediatric) from CT scan for brain examinations were the data presented as mean ± STD for the demographic information, scan chest and brain for pediatric patient (0-5) years old with total number of 105 pediatric patient the age and body mass index was 3.15 ± 1.62 years and 16.09 ± 1.50 kg/cm2 respectively, and for the radiographic data the kV was 120 for all patients and the mA, DLP, CTDIvol and ED was 756.25 ± 477.24, 43.90± 25.8 and 8 ± 5.24 respectively. Comparing the demographic and radiographic information from CT brain and chest among male and female for age, mA, DLP male has the highest values 3.31 ±1.7, 168.31± 92.58, 781.87 ±535.36 respectively,

as for BMI, CTDIv, ED this factors was high for female 16.8 ±1.8, 45.8 ±25.9, 8.3± 5.6 respectively.

Tables 4.17, 4.19, 5.21 and 4.23 shows the statistical parameters for demographic and radiological parameters for brain (pediatric) examinations as mean ± standard deviation age is almost the same for all hospitals there is no significant difference, BMI. As for mA,DLP,CTDIv Alya and Alzytona hospitals have the same values 101.3±29, 1152.8±469.8, 67.5±16.9 respectively, Ibnalhythem hospital and Modern center have the same values of mA, DLP, CTDIv 229.22 ± (21.7,223.5), 571± 66.2, 39.3 ±2.5 respectively. Ibnalhythem hospital has the highest effective dose 12.7±5.2 due to use of (4 slice) old CT scanner.

Tables 4.18, 4.20, 5.22 and 4.24 shows the statistical parameters for demographic and radiological parameters for chest (pediatric) examinations as mean ± standard deviation age was high in Alzytuona hospital 3.8 ±2,BMI is high for Modern center 17 ±1.73, mA was high for Alya hospital 310 ±189. As for DLP, CTDIv, ED this factors were high at Ibnalhythem hospital 491.2 ±187, 15.2± 2.8, 12.8 ±4.9 respectively.

Table 4.25 show the effective dose for brain and chest in all hospital for adult and pediatric, Ibnalhythem hospital has the highest ED in brain examination for adult and pediatric 10.52 mSv and 12.7 mSv also the highest ED for pediatric in chest examination for pediatric 12.8 mSv. Chest examination in adult patient has the highest ED from Alzytuona hospital 22.65 mSv.

4.2 Conclusion

This study helps to improve Occupational awareness to ionizing radiation hazard from CT procedures and the impotent of radiation protection protocols to a chive ALARA. Comparing the demographic and radiographic information from CT brain among male and female for age and BMI the age data shows the males was older than female and the body mass index data its almost similar for both gender. The radiographic data show the mA was higher for female than male while the DLP, CTDIvol and effective dose was higher for male. The demographic and radiographic information from CT chest among male and female we found that the mA for female was higher than male, while the dose length product and computed tomography dose index per volume was higher for male, the effective dose the male was higher than that from female. And when compared with diagnostic reference level and other countries found that the CTDIvol was lowest at present study between all studies except the study from UK 2013.

Patient data for both male and female (pediatric) also collected from four different hospital (same hospitals for adult patient) and centers in Khartoum which using different CT scanner modalities, comparing the demographic data and radiographic information for male and female patients from CT scan for pediatric during brain examinations, the demographic information shows age for male was higher than female, while the body mass index for female was higher than male, for the demographic data the mA, DLP and effective dose was higher for male while the CTDIvol for female was higher than male. comparing the demographic data and radiographic information for male and female patients from CT scan for pediatric during chest examinations, the demographic information the age for male was higher than female while the body mass index for female was higher than that for male, the demographic data the mA, DLP, CTDIvol and effective dose was higher for female.

4.3 Recommendations

- Special care for young female patient should be taken in chest CT.
- Using pediatric protocol for pediatric instated of adult protocol is an important factor to reduce the radiation dose and hence risk from radiation.
- Further education in radiation protection for occupational is required.

Reference

Brenner DJ, Hall EJ. Computed tomography: an increasing source of radiation exposure. N Engl J Med 2007; 357: 2277-2284.

Diana L. Miglioretti, PhD,1,2 Eric Johnson, MS,1 Andrew Williams, PhD,3 Robert T. Greenlee, PhD, MPH,4 Sheila Weinmann, PhD, MPH,5 Leif I. Solberg, MD,6 Heather Spencer Feigelson, PhD, MPH,7 Douglas Roblin, PhD,8 Michael J. Flynn, PhD,9 Nicholas Vanneman, MA,10 and Rebecca Smith-Bindman, MD11,12,13: Pediatric Computed Tomography and Associated Radiation Exposure and Estimated Cancer Risk.

European Commission. European guidelines on quality criteria for computed tomography EUR 16262 En, Luxemburg (1999).

E L NICKOLOFF, DSC and P O ALDERSON, MD; A comparative study of thoracic radiation doses from 64-slice cardiac CT(2006).

Goldman LW. Principles of CT: radiation dose and image quality. J Nucl Med Technol. 2007;35:213–225.

Hui Hua Multi-slice helical CT: Scan and reconstruction *Applied Science Laboratory, Milwaukee, Wisconsin 53201-0414(1998).*

International Commission of Radiological Protection. Recommendation of the International Commission of Radiological Protection. Biological and Epidemiological Information on Health Risk Attributable to Ionizing Radiation: A summary of Judgments for the purposes of Radiological Protection of Humans available online at http://www.icrp.org/Health_risks.pdf. Accessed on 12.04.07.

ICRP. Managing Patient Dose in Computed Tomography. s.l. : ICRP Publication 87, 2000.

Ian A. Cunningham Victoria Hospital, Philip F. Judy Harvard Medical School "Computed Tomography"(2000).

Jenia Vassileva & Madan M. Rehani & Kimberly Applegate & Nada A. Ahmed & Humoud Al-Dhuhli & Huda M. Al-Naemi: IAEA survey of paediatric computed tomography practice in 40 countries in Asia, Europe, Latin America and Africa: procedures and protocols

Mikkel Øberg; Patient Doses for CT Examinations in Denmark(2011).

Mikhail V. MALKO; Chernobyl Radiation-induced Thyroid Cancers in Belarus(2000).

M. Galanski, H.D. Nagel, G. Stamm: Paediatric CT Exposure Practice in the Federal Republic of Germany

N Buls, H Bosmans, C Mommaert, F Malchair, P Everarts, CT paediatric doses in Belgium: a multi-centre study (2010).

N Buls, Universitair Ziekenhuis Brussel H Bosmans, Universitair Ziekenhuis Leuven C Mommaert, Bel V F Malchair, Université de Liège P Clapuyt, Cliniques Universtaires Saint-Luc P Everarts, Centre Hospitalier de Jolimont-Lobbes: CT paediatric doses in Belgium: a multi-centre study.

Semens medical: Computed Tomography its History and Technology,(2011) .

Shrimpton, P.C., D.G. Jones, M.C. Hillier et al (1991). Survey of CT practice in the UK. Part Dosimetric aspects. NRPB-R249. NRPB, Chilton.

Strategies for CT radiation dose optimization. Kalra, M. K., Maher, M. M., Toth, T. L., Hamberg, L. M., Blake, M. A., Shepard, J. A. and Saini, S. 203(3):619-628, s.l. : RSNA, March 2004, Radiology.

Takeshi Kubo, Pei-Jan Paul Lin, Wolfram Stiller, Masaya Takahashi, Hans-Ulrich Kauczor Yoshiharu Ohno, Hiroto Hatabu, Radiation Dose Reduction in Chest CT: A Review(2008).

Tilo Niemann & Lucie Colas & Hans W. Roser & Teresa Santangelo & Jean Baptiste Faivre & Jaques Remy & Martine Remy-Jardin & Jens Bremerich: Estimated risk of radiation-induced cancer from paediatric chest CT: two-year cohort study

United Nations Scientific Committee on the Effects of Atomic Radiation (2000). Report to the General Assembly, Annex D Medical Radiation Exposures. United Nations, New York.

William R. Hendee and E. Russell Ritenour, Medical Imaging Physics, Fourth Edition, 2002.

Yoshito Tsushima, Ayako Taketomi-Takahashi, Hiroyuki Takei,Hidenori Otake, Keigo Endo: Radiation Exposure from CT Examinations in Japan(2010).

Patient data	***sex***	
	age	
	Wight	
	height	
Exposure parameter	***kvp***	
	mAs	
Dosimetry data	***DLP***	
	CTDIv	